Economic Geology
Vol. 92, 1997, pp. 807–826

# Brief Duration of Hydrothermal Activity at Round Mountain, Nevada, Determined from $^{40}Ar/^{39}Ar$ Geochronology

CHRISTOPHER D. HENRY,[†]

*Nevada Bureau of Mines and Geology, University of Nevada, Reno, Reno, Nevada 89557*

HALLET B. ELSON,[*]

*Round Mountain Gold Corporation, Round Mountain, Nevada 89045*

WILLIAM C. MCINTOSH, MATTHEW T. HEIZLER,

*New Mexico Bureau of Mines and Mineral Resources, Socorro, New Mexico 87801*

AND STEPHEN B. CASTOR

*Nevada Bureau of Mines and Geology, University of Nevada, Reno, Reno, Nevada 89557*

## Abstract

The Round Mountain gold-silver deposit is one of the world's largest volcanic-hosted precious metal deposits; reserves plus production total at least 16 million oz (500,000 kg) Au. The deposit occurs in ash-flow tuff that is ponded within its source caldera, along and overlying the caldera ring fracture. Host rocks have undergone propylitic, potassic, and high-level silicic and intermediate argillic alteration. These are interpreted either as a temporal sequence from early propylitic to late silicic and argillic or as a spatial progression from a potassic core outward to a propylitic halo.

$^{40}Ar/^{39}Ar$ ages determined by single crystal fusion of sanidine from host tuff and incremental heating of adularia indicate a most likely duration of hydrothermal activity of ~0.1 m.y., possibly no more than 0.05 m.y., and a maximum of 0.5 m.y. Eruption of host ash-flow tuff and caldera collapse occurred at 26.5 Ma; a late or postalteration tuff that rests upon mineralized rock is 26.0 Ma. Hydrothermal circulation is unlikely to have been established immediately after caldera collapse, so duration was probably considerably less than 0.5 m.y.

Eight adularia samples give ages between 25.94 ± 0.09 and 26.09 ± 0.05 Ma, and one is 26.20 ± 0.05 Ma; the mean of all nine is 26.03 ± 0.08 Ma. The maximum and minimum values and their uncertainties allows a duration of as much as 0.4 m.y., but for the following reasons, the longevity is probably much less. The absolute ages of seven samples that can be placed in the possible temporal alteration sequence do not correlate with that sequence. This does not disprove the temporal sequence but does indicate that alteration occurred in a time span which is not resolvable even with precise $^{40}Ar/^{39}Ar$ dating. Furthermore, all samples show flat age spectra, which themselves argue against a long, continuously active system. Kinetic studies of two adularia reveal diffusion domains with Ar closure temperatures between ~230° and ~390°C. Adularia that crystallized and remained at temperatures of 275°C, the maximum temperature inferred from fluid inclusion data, would yield age spectra with age gradients spanning the lifetime of the system. No spectra are consistent with a thermal history that incorporates sustained (>0.1 m.y.) temperatures at or above 275°C. Episodic activity to account for the one older adularia date cannot be precluded but is inconsistent with most data. Therefore, the hydrothermal system probably was active for less than the uncertainty in the ages of individual samples, possibly as little as 50,000 years.

We conclude that hydrothermal activity at Round Mountain was a brief event at ~26.0 Ma and was closely linked to caldera structure and magmatism. This activity followed initial ash-flow eruption by 0.5 m.y. and may have been driven by a ring fracture intrusion.

## Introduction

THE ROUND MOUNTAIN gold-silver deposit in Nye County, Nevada, has produced more than 4 million ounces (Moz; 124,000 kg) of gold through 1995 (Bonham and Hess, 1995). Calculated gold reserves at the beginning of 1996 were approximately 10.2 Moz (509 Mt at 0.02 oz/t). Because only approximately 65 percent of the mined gold was recovered until recently, the original endowment was at least 16 Moz Au.

The size and economic significance of the Round Mountain deposit has led to intense study that includes geologic mapping of Round Mountain and adjacent areas; analysis of the type, distribution, and origin of hydrothermal alteration; geochemical studies of magmatism and alteration; and K-Ar and $^{40}Ar/^{39}Ar$ dating of volcanism and alteration (Ransome, 1909; Ferguson, 1921; Ferguson and Cathcart, 1924; Mills, 1984; Harrington, 1985; Tingley and Berger, 1985; Berger et al., 1986; Boden, 1986, 1992; Shawe, 1986, 1995; Mills et al., 1988; Sander, 1988; Sander and Einaudi, 1990; Henry et al., 1996). These studies document a close relation between mineralization and caldera magmatism and structure. The

[†] Corresponding author: email, chenry@nbmg.unr.edu
[*] Present address: Euro-Nevada Mining Corporation, 6151 Lakeside Drive, Reno, Nevada 89511.

0361-0128/97/1949/807-20$6.00

Round Mountain deposit is located along the eastern ring fracture of a caldera that was active immediately before and probably during ore formation. The ring fracture established deep zones of high permeability that promoted circulation of hydrothermal fluids. Circulation may have been driven by a ring fracture intrusion emplaced late during the caldera cycle.

Round Mountain also figures prominently in general models of epithermal mineral deposits. It is one of the world's largest adularia-sericite or low-sulfidation gold-silver deposits. It is cited as a type example of a hot-spring precious metal deposit and used to emphasize the connection between epithermal mineralization and active geothermal systems (Berger, 1985; Berger and Silberman, 1985; Henley, 1985; Silberman and Berger, 1985; Tingley and Berger, 1985). The hot spring connection is not universally accepted. For example, Sander (1988) and Sander and Einaudi (1990) present fluid inclusion data which indicate that the maximum hydrothermal temperatures at Round Mountain were approximately 270°C, which they interpret to indicate paleodepths of about 400 m for the main orebody. In contrast, Henry et al (1996) use geologic relations and precise $^{40}Ar/^{39}Ar$ dating to argue that mineralization was indeed shallow, with some ore forming less than a few tens of meters below the paleosurface.

Round Mountain is also an ideal site to investigate the timing and duration of hydrothermal activity. The thoroughness of previous studies on geology and alteration constitute a comprehensive framework in which to examine timing. The proposed alteration sequence of Sander and Einaudi (1990), although controversial, provides a relative temporal framework with which to compare the geochronologic data. Adularia, which is well suited to precise dating by the $^{40}Ar/^{39}Ar$ method, is abundant in the deposit and formed throughout the history of alteration. Finally, the importance of Round Mountain both economically and as a type example of epithermal mineral deposits means that the results have broad implications. This study examines the geologic setting and hydrothermal alteration at Round Mountain and reports extensive new data on the precise timing of hydrothermal activity.

## Geologic Setting

### *Regional setting*

The Round Mountain deposit overlies the eastern margin of a mostly buried caldera at the western edge of the Toquima Range in the Great Basin of central Nevada (Fig. 1; Henry et al., 1996). The Toquima Range is one of many north-northeast-striking ranges separated by alluviated valleys generated by late Cenozoic extension. Central Nevada was an area of intense mid-Cenozoic ash-flow magmatism that created numerous calderas (Boden, 1986; Shawe et al., 1986; Best et al., 1989; and references in Fig. 1). At least 13 calderas that range in age between about 32 and 22 Ma have been mapped or interpreted in the Toquima Range, in the Toiyabe Range and Shoshone Mountains to the west, and in the Monitor Range to the east (Fig. 1). Several of these calderas are partly buried beneath late Cenozoic basin fill, and other calderas may be completely buried. Additional detailed mapping in the region probably will identify still more calderas.

### *The Round Mountain caldera*

The geology of the Round Mountain deposit is well understood from detailed geologic mapping, extensive drilling, and K-Ar and $^{40}Ar/^{39}Ar$ dating (Tingley and Berger, 1985; Shawe et al., 1986; Boden, 1992; Shawe, 1995; Henry et al., 1996). Henry et al. (1996) describe in detail the geology and evolution of the Round Mountain caldera. Major stratigraphic units and their ages, mostly determined by $^{40}Ar/^{39}Ar$ dating of sanidine, are listed in Table 1.

### *Pre-Round Mountain caldera rocks*

Precaldera rocks include Paleozoic sedimentary rocks, Cretaceous granite, and Eocene to Oligocene intrusive and volcanic rocks (Figs. 2 and 3; Table 1). The pre-Cenozoic rocks underlie Round Mountain and crop out extensively to the east in the Toquima Range. Deformed and locally metamorphosed Cambrian to Ordovician quartzite, limestone, and argillite were intruded by Cretaceous granitic bodies in several places in the southern Toquima Range (Shawe et al., 1986).

An extensive swarm of 34 to 37 Ma, northeast-striking, rhyolitic, andesitic, and monzonitic dikes and a small body of granodiorite cut the Cretaceous granite of Shoshone Mountain immediately east of Round Mountain (Figs. 2 and 3; Shawe et al., 1986). Petrographically similar dikes cut Paleozoic rocks beneath Round Mountain; these dikes are probably also 34 to 37 Ma but are highly altered and have not been dated.

The tuff of Dry Canyon crops out northeast of Round Mountain and appears to fill the mostly buried Dry Canyon caldera (Figs. 2 and 3; Boden, 1986; Henry et al., 1996). Drill holes that bottom in the tuff indicate a minimum thickness of 288 m northeast of Round Mountain. The tuff is densely welded, contains clasts of Paleozoic sedimentary rocks and Cretaceous granite up to 300 m long (Shawe and Snyder, 1988), and pinches out abruptly against Paleozoic rocks in outcrop to the east and in the subsurface beneath Round Mountain (Fig. 3). K-Ar (Boden, 1986) and $^{40}Ar/^{39}Ar$ dates (Henry et al., 1996) indicate that the tuff of Dry Canyon dates at 32.2 Ma, nearly 6 m.y. older than the volcanic rocks of the Round Mountain caldera. Several other pre-Round Mountain caldera ash-flow tuffs crop out in the Toquima caldera complex approximately 5 km to the northeast (Fig. 1; Boden, 1992), outside the area shown in Figure 2.

### *Tuff of Round Mountain*

The Round Mountain caldera formed at 26.5 Ma, during eruption of the tuff of Round Mountain (Henry et al., 1996). The tuff is divided into two informal members, a lower member that is more than 600 m thick, and an upper member (original tuff of Round Mountain of Tingley and Berger, 1985) that is as much as 390 m thick (Figs. 2 and 3). Both members were deposited within and against the topographic wall of the caldera. The lower member, which is encountered only in drill holes, is densely to moderately welded and contains numerous debris lenses and individual megabreccia blocks of Paleozoic rock as much as 60 m thick. The debris lenses include probable pyroclastic fall and surge deposits, as well as breccia shed from the caldera wall. The tuff is mostly a single cooling unit, but the fall and surge deposits indicate

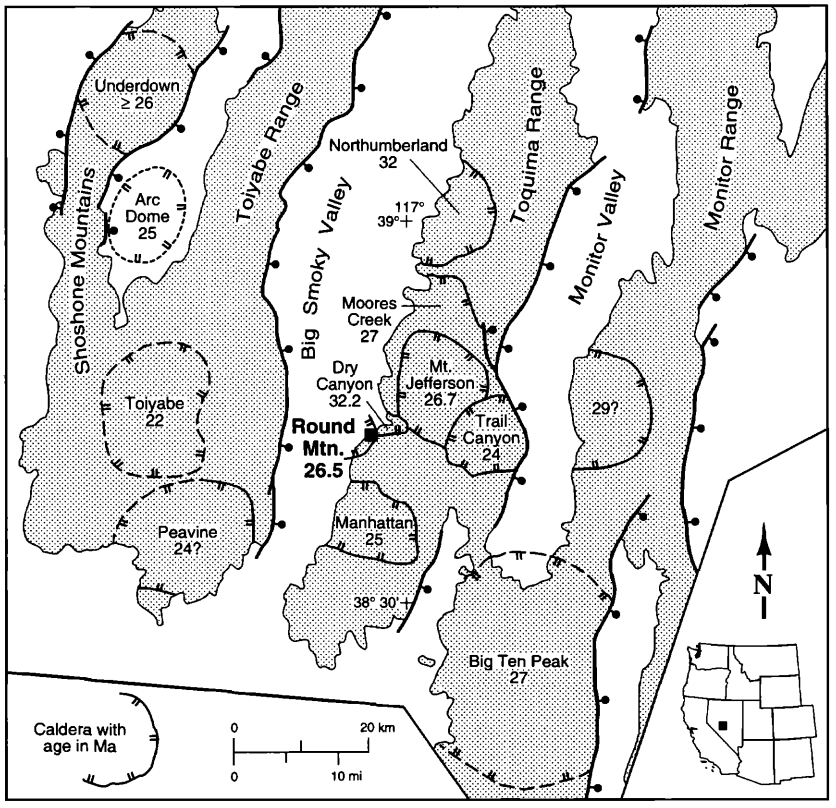


FIG. 1. Regional geologic setting of the Round Mountain gold deposit. Round Mountain lies at the western edge of the Toquima Range, one of numerous north-northeast-trending ranges in the central Great Basin of Nevada. At least 13 mid-Tertiary calderas occur within the Toquima Range and adjacent Shoshone Mountains and Toiyabe and Monitor Ranges. Round Mountain lies at the eastern edge of the Round Mountain caldera, which extends westward into Big Smoky Valley. Data from McKee (1974, 1976), Stewart and Carlson (1978), Brem and Snyder (1983), Snyder and Healey (1983), Kleinhampl and Ziony (1985), Tingley and Berger (1985), Boden (1986, 1992), Shawe et al. (1986), Shawe and Snyder (1988), Best et al. (1989), Brem et al. (1991), John (1992), Plouff (1992), Shawe (1995), and Henry et al. (1996).

breaks during eruption, particularly in the upper part. The tuff wedges out northeastward against Paleozoic rocks beneath Round Mountain and thickens markedly to the west as the top of the Paleozoic rocks drops steeply (section A-A'; Fig. 3). The steep, southwest-dipping contact of the lower member with pre-Cenozoic rocks in Figure 3 must coincide closely with the caldera ring fracture. The more gentle contact to the northeast along section A-A' dips too shallowly to be

TABLE 1. Stratigraphy at Round Mountain, Nevada

| Informal name | Members | Rock type | Thickness (m) | Age (Ma) |
|---|---|---|---|---|
| Tuff of Big Smoky Valley | | Densely welded ash-flow tuff | 23–30 | **26.07 ± 0.05**[2]<br>**25.93 ± 0.15**[2] |
| Stebbins Hill sequence | | Volcaniclastic, lacustrine sedimentary rocks; air-fall and ash-flow tuff | 91 | |
| Tuff of Round Mountain | Upper member[1] | Densely welded ash-flow tuff | 220 | **26.50 ± 0.06** |
| | | Nonwelded ash-flow tuff | 50–210 | **26.54 ± 0.07**<br>**26.48 ± 0.08**<br>**26.52 ± 0.15** |
| | Lower member | Densely welded ash-flow tuff | >600 | **26.53 ± 0.07** |
| Tuff of Dry Canyon | | Coarsely lithic ash-flow tuff | | **32.18 ± 0.13** |
| | | Rhyolitic to andesitic dikes | | 34 to 37 |
| Granite of Shoshone Mountain | | | | Cretaceous |
| Paleozoic Sedimentary Rocks | | | | Cambrian-Ordovician |

Ages in bold are $^{40}Ar/^{39}Ar$ determinations from Henry et al. (1996); other ages are from Shawe et al. (1986)
[1] Original tuff of Round Mountain of Tingley and Berger (1985)
[2] Mean and isochron ages, respectively, of a single sample

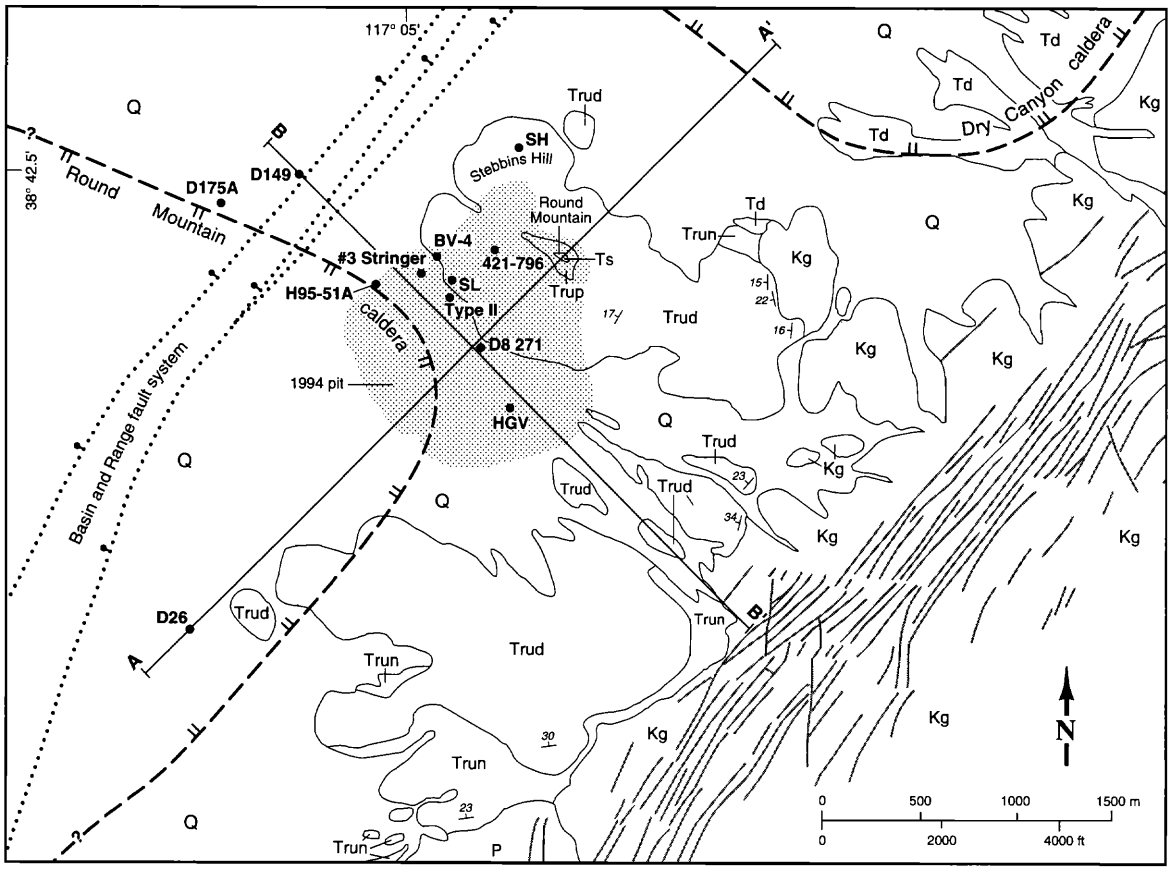


FIG. 2. Geologic map of the Round Mountain mine area before mining (modified from Boden, 1992, and Shawe, 1995) showing approximate location of ring fractures of the Round Mountain and Dry Canyon calderas, late Basin and Range faults, cross sections, sampled drill holes, and sample locations (including extrapolation to surface of samples from drill holes or pit). See Figure 3 for explanation.

a caldera boundary fault so it is most likely a scarp eroded along the fault. These characteristics indicate that the lower member fills the Round Mountain caldera, which collapsed during its eruption, and that part of the tuff was deposited against the caldera wall outside the ring fracture.

The upper member of the tuff of Round Mountain forms a single cooling unit separated from the lower member by a distinct cooling break (Figs. 2 and 3). Most of the upper member consists of a lower, nonwelded part and an overlying, densely welded tuff. Poorly welded, vapor phase-altered tuff formerly cropped out above the densely welded tuff near the top of Round Mountain (Figs. 2 and 3; Tingley and Berger, 1985; Sander, 1988); it has been removed by mining but is preserved on the downthrown side of a system of northeast-striking Basin and Range faults west of Round Mountain (section B-B'; Fig. 3). Coarse, massive debris lenses containing clasts of pre-Cenozoic rocks up to several meters in diameter are common in the lower, nonwelded part and are exposed in the pit.

The upper member wedges out eastward against a moderately steep paleoslope developed on pre-Cenozoic rocks and the tuff of Dry Canyon (section A-A'; Fig. 3). The upper member thickens gradually southwestward into the caldera. It is about 290 m thick at Round Mountain and thickens to at least 390 m about 1,300 m southwest of Round Mountain, where the top is eroded. Most of the thickening occurs within the lower, nonwelded part, which is 98 m thick below Round Mountain and more than 210 m thick almost directly above the ring fracture. The nonwelded part then thins southwestward and becomes more welded. The stratigraphic equivalent of the nonwelded tuff in drill hole D26 at the southwestern end of section NE-SW (Fig. 3) is no more than 50 m thick and is poorly to moderately welded.

These field characteristics indicate that the upper member was deposited along the eroded caldera wall, shortly after emplacement of the lower member, while the wall still had considerable relief but after most, possibly all, collapse had occurred. The cooling break between the two members is most distinct at the caldera wall, which was probably a heat sink that promoted rapid cooling. The less pronounced cooling break within the caldera suggests that the lower member was still moderately hot at the time of deposition of the upper member.

Both members contain abundant phenocrysts of sanidine, plagioclase, and quartz, with lesser biotite, hornblende, Fe-Ti oxides, and zircon. The lower member contains 30 to 40 percent phenocrysts. Phenocryst abundance in the upper member increases upward from less than 10 to more than 40

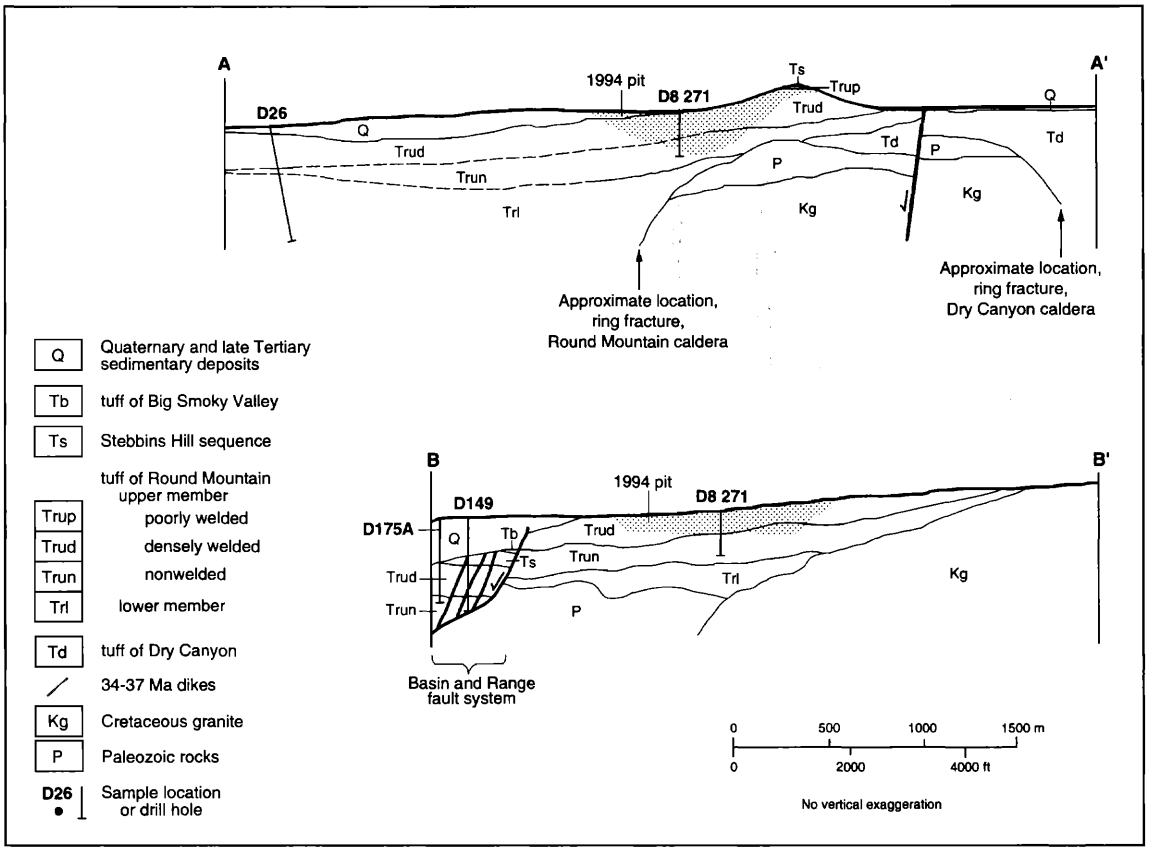


FIG. 3. Cross sections across the Round Mountain deposit; see Figure 2 for location. Sections are based on extensive drilling, but only sampled drill holes are shown. Section A-A′: the tuff of Round Mountain, including the upper member (original tuff of Round Mountain; Tingley and Berger, 1985) and lower member, is ponded within and rests upon pre-Cenozoic rocks in the topographic wall of the Round Mountain caldera. The caldera ring fracture is approximately coincident with the steep southwest-dipping contact between the lower member and pre-Cenozoic rocks. Ring fracture of Dry Canyon caldera is probably just northeast of steep contact of tuff of Dry Canyon with pre-Cenozoic rocks. Section B-B′: several northeast-striking Basin and Range faults drop the tuff of Round Mountain, Stebbins Hill sequence, and tuff of Big Smoky Valley down to the northwest.

percent, reflecting a combination of compaction and compositional zoning, with the tuff becoming slightly less silicic upward (Boden, 1986).

Five $^{40}Ar/^{39}Ar$ ages determined on the lower and upper members of the tuff of Round Mountain range from 26.48 ± 0.08 to 26.54 ± 0.07 Ma with a mean of 26.51 ± 0.03 Ma (Henry et al., 1996; Table 1). The ages of the two members are indistinguishable; this is consistent with the field data which indicate that the two members erupted closely in time from the Round Mountain caldera.

*Intracaldera sediments: Stebbins Hill sequence*

The Stebbins Hill sequence of volcaniclastic rocks and minor ash-flow and pyroclastic-fall tuff overlies the tuff of Round Mountain. These rocks are preserved only beneath late Tertiary and Quaternary basin-fill deposits on the downthrown side of the Basin and Range faults where they are as much as 91 m thick (Fig. 3). However, about 8 m of the lowermost part of the Stebbins Hill sequence capped Round Mountain before mining (Tingley and Berger, 1985). The sedimentary rocks include tuffaceous sandstone, pebbly to coarse conglomerate, and lacustrine deposits of thinly laminated, planar-bedded siltstone and clay. These rocks accumulated within the closed caldera basin following the end of major eruption. The considerable thickness of the Stebbins Hill sequence demonstrates a significant hiatus between emplacement of the tuff of Round Mountain and the overlying tuff of Big Smoky Valley, consistent with the approximately 0.5-m.y. difference in ages (Table 1).

The Stebbins Hill sequence has undergone argillic alteration and locally is intensely silicified. Gold-bearing veins cut the sedimentary rocks, and much of the sequence is of ore grade and will be mined. Controversy exists over the presence and significance of sinter in the Stebbins Hill sequence, which bears on the timing of hydrothermal activity. The thin interval that formerly capped Round Mountain was intensely silicified, brecciated, and recemented with quartz (Berger, 1985; Tingley and Berger, 1985). Tingley and Berger (1985) and B.R. Berger (pers. commun., 1995) report clasts of thinly laminated chalcedonic sinter in what they interpret to be hydrothermal explosion breccia formed no more than 100 m below the paleosurface. However, Sander and Einaudi (1990) argue that any sinter in the Stebbins Hill sequence would have been several hundred meters below the paleosurface

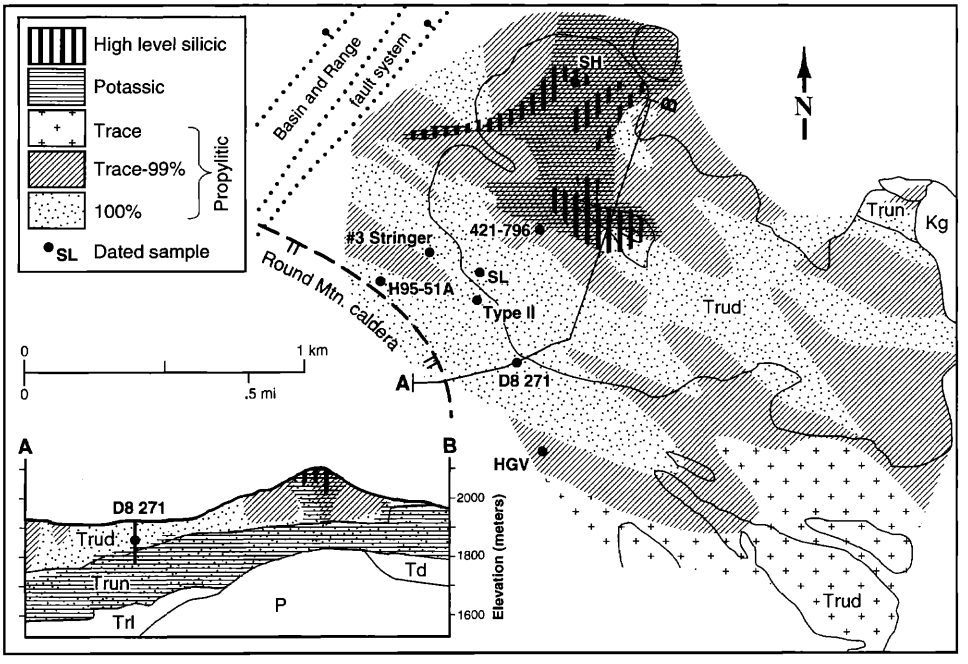


FIG. 4. Distribution of hydrothermal alteration of the upper member of the tuff of Round Mountain from Sander and Einaudi (1990; their fig. 4) superimposed on part of geologic map of Figure 2. They interpreted propylitic, potassic, and high-level silicic alteration to have occurred sequentially in that order. Intensity of propylitic alteration is defined by degree of replacement of sanidine phenocrysts by adularia. Fluids that generated propylitic alteration were channeled along northwest-striking faults and joints, which are marked by linear bands of 100 percent replacement. The transition to potassic alteration resulted from abrupt flushing with cold ground water. Potassic and high-level silicic alteration were superimposed on propylitic alteration. Dated adularia samples span the range of the proposed alteration sequence (Table 2).

and therefore not related to the ore-forming system. Silica-rich lenses in drill core examined by us are probably silicified tuff and sediment rather than subaerially or subaqueously deposited sinter.

*Late or postalteration tuff of Big Smoky Valley*

The youngest unit at Round Mountain, the rhyolitic tuff of Big Smoky Valley, is also only preserved on the downthrown side of the Basin and Range faults. The tuff has a densely welded basal vitrophyre that passes upward into densely welded, devitrified rock. It is as much as 30 m thick, but erosion that preceded Basin and Range faulting stripped it from much of the area (Fig. 4). The rock is sparsely and finely porphyritic, with 5 to 10 percent phenocrysts, mostly of plagioclase with less abundant sanidine, biotite, quartz, Fe-Ti oxides, and zircon.

Mean and isochron ages of sanidine from the tuff of Big Smoky Valley (sample D22-837) are 26.07 ± 0.05 and 25.93 ± 0.15 Ma, respectively (Table 1). These are indistinguishable given the combined uncertainties, and the best estimate of the tuff's age is probably 26.0 Ma, the average of the mean and isochron ages.

The source of the tuff of Big Smoky Valley and its relation either to the Round Mountain caldera or to other calderas in the region are uncertain (Henry et al., 1996). The tuff could be a late eruption from the Round Mountain caldera or a distal deposit from a distant caldera.

Most of the tuff of Big Smoky Valley is unaltered. However, nonwelded tuff at the base of the unit is bleached and limonitic. Petrographic and X-ray analyses show that alteration products include montmorillonite, opal, and cristobalite. The significance of this alteration is uncertain. It could be a late phase of alteration related to the gold-depositing system, possibly the late, high-level silicic alteration of Sander and Einaudi (1990). Alternatively, it could represent a much later event that has no connection with gold deposition. By either interpretation, the tuff could have been emplaced no earlier than at the end of alteration of the gold system.

*Geometry of the Round Mountain caldera*

Extensive drilling around Round Mountain allows delineation of an arcuate ring fracture system over a distance of about 6 km beneath the deposit (Figs. 2 and 3; Henry et al., 1996). However, the continuation of the caldera westward into Big Smoky Valley is poorly understood. The caldera does not extend into the eastern part of the Toiyabe Range (Fig. 1), because Paleozoic sedimentary rocks crop out there (Whitebread and John, 1992). This limits the caldera diameter to about 11 km. The lower and upper members of the tuff of Round Mountain are either flat lying or dip gently southwestward where exposed or encountered in drilling. Therefore, either the caldera was not resurgent, or resurgence affected only a small area in the middle of the caldera, which has not been examined.

*Alteration assemblages at Round Mountain*

An understanding of the geometry and history of alteration at Round Mountain is critical to evaluating the duration of

TABLE 2. Alteration Sequence and Temperatures of Sander and Einaudi (1990)

| | Alteration | T (°C) | | Adularia occurrence | $^{40}Ar/^{39}Ar$ samples |
|---|---|---|---|---|---|
| Late | High-level silicic | ≤180 | | Coxcomb veins | SH |
| | High-level argillic | ≤180 | | None | |
| | Potassic | 250 to 150 | Main ore deposition | Open-space, groundmass | HGV, SL, Type II[1] |
| | (transition) | | | Overgrowth veins | #3 Stringer |
| Early | Propylitic | 250 to 270 | | Adularized sanidine | D8 271, H95-51A |

[1] Samples D175A and 421-796 are probably also from potassic alteration

hydrothermal activity. Unfortunately, although the geometry of alteration is well understood, its temporal significance is debated. In a comprehensive study of the alteration of the upper member of the tuff of Round Mountain, Sander (1988) and Sander and Einaudi (1990) identified propylitic, potassic, and high-level silicic and intermediate argillic assemblages (Fig. 4; Table 2). Furthermore, they interpreted these to have formed sequentially in that order. In contrast, Tingley and Berger (1985), current mine geologists, and others (H. F. Bonham, Jr., pers. commun., 1995) consider the same assemblages to be a spatial progression from a potassic core outward to a propylitic halo, all of which formed approximately at the same time. Nevertheless, the temporal interpretation of Sander (1988) and Sander and Einaudi (1990) is potentially testable using $^{40}Ar/^{39}Ar$ dating, so we review their work as a framework in which to discuss our ages.

Propylitic alteration is characterized by the mineral assemblage quartz-adularia-albite-chlorite-calcite-pyrite-rutile ± epidote. According to Sander and Einaudi, adularia formed only by replacement of sanidine phenocrysts during propylitic alteration. They defined zones of different intensity on the basis of degree of replacement (Fig. 4); the most intense zones coincide with northwest-striking faults and joints that probably channeled hydrothermal fluids. Propylitic alteration resulted from circulation of a low-salinity fluid with maximum temperature between 250° and 270°C (see also Berger, 1985). Although the relationship of early propylitic alteration to ore mineralization is unclear in many precious metal districts, Sander and Einaudi (1990) concluded that propylitic alteration at Round Mountain was an early manifestation of the ore-forming hydrothermal system and essential in developing bulk mineable ore.

Most gold deposition occurred during the transition from propylitic to potassic alteration, when hydrothermal temperatures dropped from about 250° to 150°C at constant pH and $f_{O^2}$ (Sander and Einaudi, 1990). They relate the transition to lateral incursion of cold ground water resulting from fracturing during regional extension. Overgrowth veins, in which adularia precipitated over sanidine phenocrysts, formed in the densely welded upper member tuff during the transition. Otherwise, potassic alteration is best developed in poorly welded tuff (Fig. 4).

Late silicic and intermediate argillic alterations, which are dominantly postore, resulted from further cooling with temperatures less than 180°C. These formed only at high levels in the Round Mountain system (Fig. 4). Minor alteration that affected the tuff of Big Smoky Valley could be a part of the late silicic phase. Sander and Einaudi (1990) emphasize that hydrothermal alteration was a continuous process interrupted only by the sudden influx of cold ground water which quenched the system and deposited gold. A possible implication of their model is that propylitic alteration could have been protracted, whereas the rest of the alteration sequence is likely to have been brief.

Adularia formed throughout this proposed alteration sequence (Table 2). Adularia replaced sanidine phenocrysts during propylitic alteration. Overgrowth veins containing coarse adularia formed during the transition from propylitic to potassic alteration. During potassic alteration, coarse-grained adularia precipitated in veins and in cavities in tuff, and fine-grained adularia replaced groundmass. Coxcomb quartz-adularia veins formed during late silicification in the upper parts of Round Mountain.

## $^{40}Ar/^{39}Ar$ Methodology

### *Samples*

$^{40}Ar/^{39}Ar$ dating was done on adularia collected to encompass the proposed alteration sequence and throughout the deposit to test spatial variations (Table 2; Fig. 4; Appendix). These include two samples of adularia that has completely replaced sanidine (D8 271 and H95-51A), a sample from an overgrowth vein (#3 Stringer), three samples from potassic alteration (HGV, Type II, and SL), and one sample of a late, coxcomb vein (SH). All seven samples are hosted by the upper member of the tuff of Round Mountain. Assignment to the Sander and Einaudi (1990) alteration sequence is based upon matching their textural types and distribution of assemblages and, for two samples (D8 271 and #3 Stringer), specific citation. Two additional samples (421-796 and D175A) probably formed during potassic alteration. However, sample D175A, from the upper member, lies northwest of the Basin and Range faults, outside the area examined by Sander and Einaudi (1990), and also underwent propylitic alteration. Sample 421-796 is from Paleozoic rocks that underlie a thin wedge of the lower member. The Paleozoic rocks also may have undergone propylitic alteration, but the fine-grained shale lacks diagnostic alteration minerals. Crosscutting relations to determine relative ages for the samples are few, which is part of the reason company geologists are skeptical of the proposed temporal sequence.

Adularia occurs as three textural types: replaced sanidine; coarse, open-space-filling grains; and fine replacement of groundmass (Fig. 5). Adularia replacing sanidine forms a coarse mosaic that mimics the original phenocryst and can only be distinguished from unaltered sanidine in hand speci-

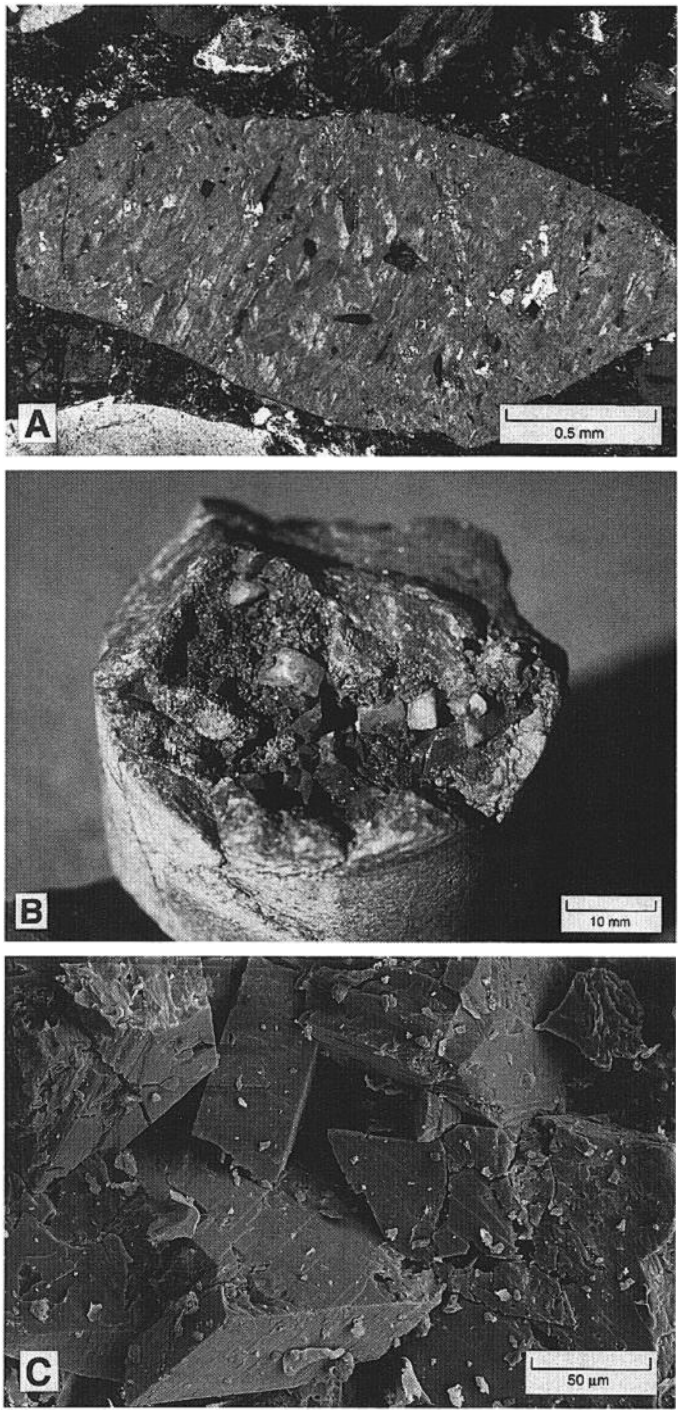


FIG. 5. A. Sanidine phenocryst replaced by adularia showing characteristic mottled extinction (sample H95-51A). Note inclusions of calcite, albite, and smectite. Dated separate consists of former individual phenocrysts. B. Coarse adularia rhombs up to 5 mm across (core sample 421-796, a vein in Paleozoic rocks). Dated separate consists of individual crystals. C. SEM photograph of fine-grained adularia, approximately 50 μm across and intergrown with quartz, that replaced groundmass in lower nonwelded part of the lower member of tuff of Round Mountain (sample SL).

mens by a slight cloudiness. In thin sections, adularized phenocrysts are easily identified by mottled extinction (Fig. 5A). Coarse adularia coats fractures and fills voids left from alteration of pumice and ranges up to about 7 mm in diameter (Fig. 5B). Coarse adularia is commonly milky white from abundant fluid inclusions. Fine adularia replaces groundmass or pumice, especially in nonwelded ash-flow tuff of the upper member, and occurs in grains ranging from about 1 to 200 μm in diameter (Fig. 5C). In some samples (e.g., SL), fine adularia occurs as a mosaic with quartz and sericite that almost completely obscures original textures. Analyses by scanning electron microscope show that coarse and fine adularia are nearly end-member K feldspar (Table 3). However, adularized sanidine typically contains 1.5 wt percent $Na_2O$ ($\sim Or_{87}$ $Ab_{13}$), possibly retained from the sanidine phenocrysts, which originally contained about 4 wt percent $Na_2O$ (Henry et al., 1996).

*Sample preparation*

Samples containing adularized sanidine phenocrysts were crushed and sieved to 20 to 40 mesh, then run through a magnetic separator to concentrate feldspar and quartz phenocrysts. Individual adularized phenocrysts were hand picked and leached with dilute HF to remove coating groundmass.

Coarse adularia grains were hand picked from cavities or selvages. The grains were leached with dilute HF and separately with nitric acid to remove common iron oxyhydroxide coatings. The resulting adularia samples were sieved to less than 10 mesh and consist mostly of individual crystals.

Fine adularia in samples SL and HGV was concentrated by crushing the rock and sieving to 80 to 100 mesh. Magnetic material, mostly groundmass and alteration products containing iron oxides, was removed with a magnetic separator. After leaching with dilute HF, samples were separated into five to six density fractions by progressive settling in diluted bromoform. Grain mounts of these fractions were examined with a petrographic microscope. The most adularia-rich aliquots were then further concentrated by magnetic and density separation.

Petrographic and SEM examinations indicate that all adularia contains fluid and mineral inclusions, most of which are also products of hydrothermal alteration. Adularized phenocrysts contain quartz, albite, and probable smectite and chlorite (Fig. 5A). Adularized sanidine in sample H95-51A also contains calcite. Coarse adularia contains sparse quartz inclusions, and fine adularia is intergrown with quartz; however, quartz constitutes no more than about 1 percent of the analyzed samples.

*Isotopic analysis*

Samples were irradiated in two batches at the University of Michigan (10 h) or Texas A&M University (6 h) and analyzed at the New Mexico Bureau of Mines and Mineral Resources. Fish Canyon sanidine (27.84 Ma, relative to an age of 520.4 Ma on hornblende from sample MMhb-1; Cebula et al., 1986; Samson and Alexander, 1987) was used to monitor neutron fluence. Samples were heated in a resistance furnace, and released gas was purified using SAES getters.

Two samples (H95-51A and D175A) were studied in detail to determine their kinetic properties, overall gas release pattern, and nonradiogenic Ar contents. These samples were heated in 21 steps of variable duration between 450° to 550°C and 1,650°C. Gas fractions released below about 750°C

TABLE 3. Representative Analyses of Adularia by Energy-Dispersive Scanning Electron Microscope

| | Adularized sanidine | | Overgrowth vein | Replacement of: | | |
|---|---|---|---|---|---|---|
| | | | | Groundmass | Pumice | Plagioclase |
| Alteration type | Propylitic | | Transition | Potassic | Potassic | Potassic |
| Sample no. | D8 271 | H95-51A | #3 Stringer | SL | BV-4 | D149-1528 |
| $SiO_2$ | 63.62 | 63.68 | 65.04 | 65.06 | 64.92 | 64.92 |
| $Al_2O_3$ | 18.93 | 18.86 | 17.75 | 17.62 | 17.92 | 17.71 |
| $K_2O$ | 15.40 | 15.35 | 16.42 | 16.69 | 16.37 | 16.72 |
| $Na_2O$ | 1.47 | 1.52 | <0.30 | <0.30 | 0.15 | <0.30 |
| CaO | <0.10 | <0.10 | 0.20 | <0.10 | 0.10 | <0.10 |
| FeO | 0.10 | 0.12 | 0.21 | 0.22 | 0.30 | 0.18 |
| BaO | 0.48 | 0.47 | 0.23 | 0.22 | 0.24 | 0.26 |
| Orthoclase | 87 | 87 | 99 | 100 | 98 | 100 |
| Albite | 13 | 13 | <1 | <1 | 1 | <1 |
| Anorthite | <1 | <1 | 1 | <1 | 1 | <1 |

Analyses used a JEOL 8405 scanning electron microscope equipped with a KEVEX energy dispersive analyzer (using mineral standards and Quantex VI analytical software).

mostly contained less than 1 percent of the total $^{39}Ar$ released but ranged as high as 9 percent. They also commonly had low radiogenic yields and K/Ca ratios. These low-temperature fractions appear to include a large contribution of gas from fluid inclusions (mostly atmospheric Ar) or nonadularia alteration phases (see discussion below). They contribute little information about age. For this reason, all other adularia samples were first degassed at about 600°C and then heated in ten to thirteen 10-min increments between about 700° and 1,650°C. Calculated ages are listed in Table 4 and representative spectra are shown in Figure 6.

Flux monitors and individual sanidine phenocrysts from volcanic rocks were analyzed by fusion using a $CO_2$ laser. Calculated ages (Table 1) are the mean of analyses of 6 to 12 grains. Henry et al. (1996) discuss analytical methods and results of the sanidine dating in more detail.

## General Interpretation of the $^{40}Ar/^{39}Ar$ Data

### *Kinetic properties, and range and proportion of closure temperatures*

Thermochronometric studies of adularia were conducted to help determine the thermal history of the Round Mountain hydrothermal system. These studies have been extensively applied to igneous and metamorphic K feldspars and can be extended to hydrothermal adularia. Thermochronologic methods rely on knowledge of a mineral closure temperature. A closure temperature is the temperature at which the radio-

TABLE 4. $^{40}Ar/^{39}Ar$ Ages of Adularia, Round Mountain, Nevada

| | | | | | Plateau age (Ma) | | Isochron ages (Ma) | | | | | |
|---|---|---|---|---|---|---|---|---|---|---|---|---|
| Sample no. | Description | Alteration | Irradiation batch[1] | No. of steps | ±1σ | | Plateau steps | ±1σ | $^{40}Ar/^{36}Ar_i$[2] | Low-T steps | ±1σ | $^{40}Ar/^{36}Ar_i$[2] |
| 421-796 | Vein in Paleozoic rock | Potassic? | NM-13 | 19 | **26.02** | 0.08 | **25.98** | 0.08 | 289.9 ± 1.3 | | | |
| D175A | Deep Round Mtn. | Potassic? | NM-33 | 21 | **26.20** | 0.05 | **26.25** | 0.04 | 293.3 ± 4.8 | 26.55 | 0.10 | 294.6 ± 1.5 |
| SH | Coxcomb vein | Silicic | NM-13 | 13 | **25.95** | 0.09 | **25.95** | 0.08 | 295.9 ± 1.7 | | | |
| SL | Replaces groundmass | Potassic | NM-13 | 10 | **26.05** | 0.09 | **26.02** | 0.08 | 298.3 ± 1.4 | | | |
| HGV | Vein in poorly welded | Potassic | NM-13 | 11 | **26.01** | 0.09 | **26.01** | 0.08 | 295.1 ± 8.9 | | | |
| | | | NM-33 | 12 | **26.08** | 0.06 | **26.09** | 0.09 | 07.1 ± 29.1 | 26.01 | 0.06 | 253.6 ± 2.1 |
| | | | NM-33 | 12 | **26.17** | 0.05 | **26.22** | 0.05 | 58.5 ± 25.6 | 26.01 | 0.05 | 234.0 ± 2.4 |
| Mean | | | | | **26.09** | 0.08 | **26.11** | 0.11 | | | | |
| Type II | Replaces pumice | Potassic | NM-13 | 10 | **25.94** | 0.09 | **25.96** | 0.08 | 292.6 ± 1.1 | | | |
| #3 Stringer | Overgrowth vein | Transition | NM-13 | 25 | **26.00** | 0.08 | **26.00** | 0.08 | 296.0 ± 1.9 | 26.13 | 0.12 | 295.7 ± 2.4 |
| D8 271 | Adularized sanidine | Propylitic | NM-33 | 13 | **25.95** | 0.05 | **25.95** | 0.07 | 295.5 ± 3.8 | 25.99 | 0.11 | 288.1 ± 2.3 |
| H95-51A | Adularized sanidine | Propylitic | NM-33 | 21 | **26.08** | 0.06 | **26.37** | 0.07 | 262.0 ± 7.0 | 26.02 | 0.08 | 281.7 ± 1.4 |
| Mean of nine ages | | | | | **26.03** | 0.08 | **26.07** | 0.15 | | | | |

$\lambda\beta = 4.963 \times 10\text{-}10\ yr^{-1}$; $\lambda\epsilon + \epsilon' = 0.581 \times 10\text{-}10\ yr^{-1}$; 40K/K = $1.167 \times 10^{-4}$; Steiger and Jäger (1977); values in bold = best age estimates

[1] NM-13 = Michigan; NM-33 = Texas A&M

[2] $^{40}Ar/^{36}Ari$ = trapped Ar composition

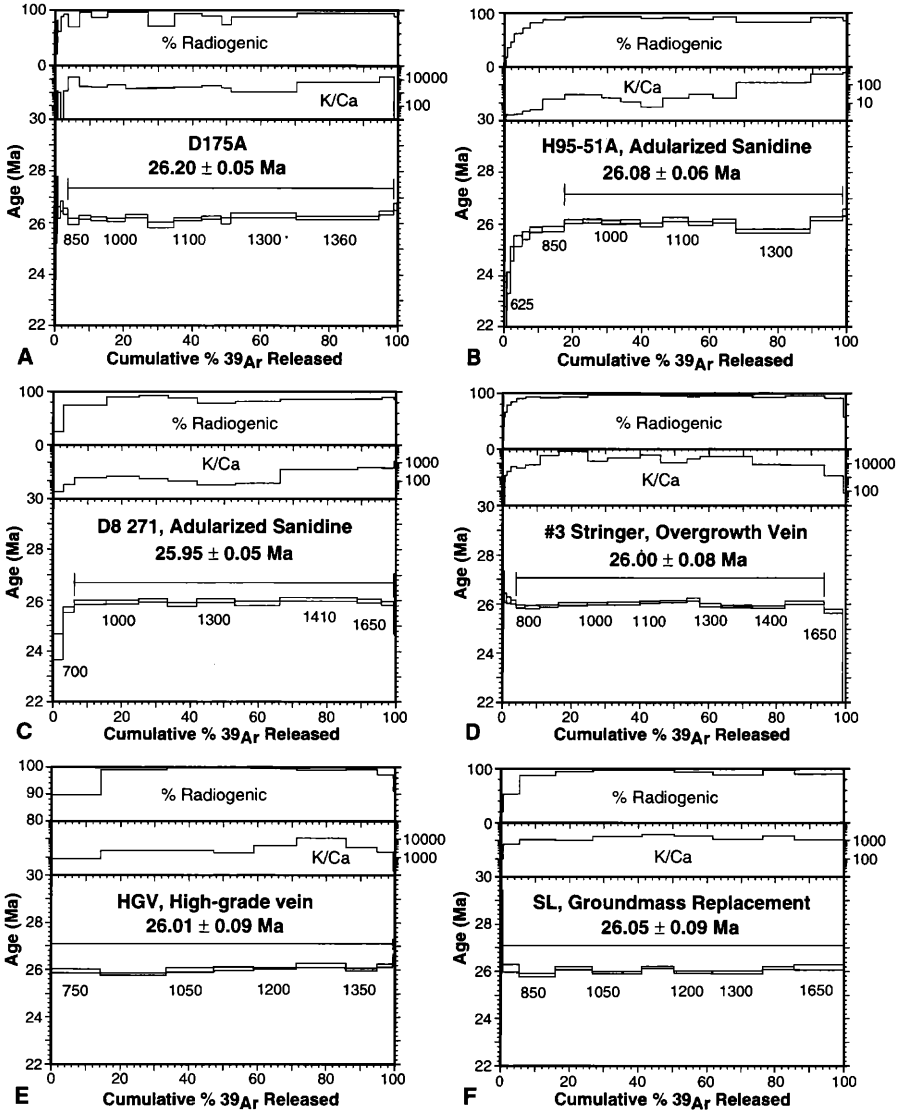


FIG. 6. Representative $^{40}Ar/^{39}Ar$ age spectra from incremental heating of adularia from the Round Mountain mine. Numbers below age spectra are incremental-heating temperatures. Ages generally were calculated from higher temperature steps, which have uniformly high K/Ca and radiogenic Ar contents. Except for adularized sanidines, only steps with K/Ca > 500 were used in age calculation. See text for further discussion. A. D175A, coarse adularia probably from potassic alteration. Low-temperature steps have low and irregular radiogenic Ar contents and K/Ca, which indicates that released gas is mostly not from adularia. Higher temperature steps, which are used to calculate a best age, have uniformly high K/Ca and mostly high radiogenic Ar contents. B. H95-51A, adularized sanidine from propylitic alteration. Low-temperature steps have low radiogenic contents and K/Ca. Higher temperature steps have K/Ca between 5 and 35, which indicates contemporaneous degassing of calcite inclusions. C. D8 271, adularized sanidine from propylitic alteration. K/Ca is low but slightly higher than in sample H95-51A and may also indicate degassing of calcite. D. #3 Stringer, coarse adularia from overgrowth vein, transition between propylitic and potassic alteration. E. HGV, fine adularia from low-angle vein formed during potassic alteration. Sample was degassed at 600°C to remove low-temperature gas. High-temperature steps yield flat spectrum with consistently high radiogenic content and K/Ca. F. SL, fine adularia that replaced groundmass in nonwelded part of upper member of tuff of Round Mountain. Sample was degassed at 600°C. High-temperature steps yield flat spectrum with consistently high radiogenic content and K/Ca.

genic daughter product ceases to diffuse from the mineral (Dodson, 1973). Kinetic properties (and thus closure temperatures) are strongly dependent upon the mineral and isotopic system and less dependent on the cooling rate or mineral composition.

Argon closure in K feldspar is treated on an individual basis following the multiple diffusion domain model method developed by Lovera et al. (1989). This model views K feldspar as containing a discrete distribution of diffusion-length scales (domains), which imparts multiple argon closure temperatures within a single sample. Because of the domainal nature of K feldspar a continuous record of the thermal history, typically between about 150° to 350°C, may be recorded within the sample. That is, small diffusion domains will pro-

vide information about the low-temperature history, and the higher temperature history will be given by the larger diffusion domains.

The closure temperatures for K feldspar are determined from the release of $^{39}Ar$ in the laboratory. Therefore, extracting meaningful thermal histories from K feldspar argon results relies on the fundamental assumption that the release of argon in the laboratory occurs by the same mechanism and is controlled by the same boundaries as in nature. High degrees of alteration and porosity (Parsons et al., 1988; Burgess and Parsons, 1994), formation of K-bearing fluid inclusions (Burgess et al., 1992; Turner and Wang, 1992; Harrison et al., 1993), laboratory-induced problems (Foland, 1994), or substantial modification of the domains at low temperature would manifest themselves by geologically irrelevant and/or internally inconsistent thermal histories. Several studies confirm a good correlation between the argon kinetics derived using the multiple diffusion domain method and age spectra for most K feldspars (e.g., Lovera et al., 1989, 1991, 1993; Leloup et al., 1992; FitzGerald and Harrison, 1993; Harrison et al., 1994; Lee, 1995). The strongest argument in support of the multiple diffusion domain method is that nearly identical and geologically reasonable thermal histories have been obtained from adjacent samples which display highly contrasting argon kinetic parameters (Heizler et al., 1988; Lovera et al., 1989; Heizler and Harrison, 1992; Leloup et al., 1992).

The domain distribution and kinetic properties of adularia samples D175A and H95-51A (Table 5) were determined from multiple diffusion domain modeling of the laboratory release of $^{39}Ar$ assuming a plane slab geometry (Lovera et al., 1989). Combining the kinetic parameters with an input thermal history allows calculation of a model age spectrum.

Kinetic properties of samples D175A and H95-51A are similar, with small but important differences (Table 5). Activation energies of 55.0 and 53.5 kcal/mole are analytically indistinguishable, and the samples have similar ranges of closure temperatures, ~260° to 390°C for D175A and ~225° to 370°C for H95-51A. The main difference in the domain distribution between the two samples is that D175A has only ~3 percent of its domains with closure temperatures below ~275°C whereas H95-51A has about 14 percent of this diffusion length scale. The implication of these data is that adularia from sample H95-51A would lose significantly more argon than that from D175A if the samples resided for a significant time at ~275°C, the maximum hydrothermal temperature at Round Mountain inferred from fluid inclusions (Sander and Einaudi, 1990).

These differences in kinetic properties may reflect differences in adularia habit between the two samples: coarse (≥1 mm), single crystals in sample D175A versus replaced sanidine phenocrysts in sample H95-51A. Adularia in the replaced phenocrysts shows mottled extinction (Fig. 5A) that may be related to an increase in smaller diffusion domains for this sample. The adularia is probably a composite of many small crystals rather than a single crystal the size of the sanidine phenocryst. Additional study of different forms of adularia would be useful to test these possibilities and to help understand the thermal history of hydrothermal systems in general.

*Plateau and inverse isochron ages*

Ages from incremental heating experiments were calculated in two ways: a variation of the plateau method, which considers only the age and analytical uncertainty of individual, contiguous steps (e.g., Fleck et al., 1977); and the inverse isochron method (McDougall and Harrison, 1988; Deino and Potts, 1990). With two exceptions, plateau ages reported here (Table 4) are weighted means, using the inverse variance as the weighting factor, of steps that have both a K/Ca ratio greater than 500 and a radiogenic yield greater than 80 percent. These requirements were used for the following reasons. All but the lowest and highest temperature parts of the age spectra were flat (Fig. 6). Low-temperature fractions invariably had low K/Ca ratios (to less than 1), a low radiogenic yield, and commonly low ages; all increased with increasing temperature. The highest temperature fractions (≥1,650°C) were more variable, but those with negligible $^{39}Ar$ also gave discordant data. Temperature fractions between these two extremes represent 80 to 99 percent of the $^{39}Ar$ released and had much higher K/Ca ratios (several hundred to ~15,000) and yields. Adularia, a nearly pure K feldspar, should have high K/Ca ratios. The K/Ca cutoff value of 500 is somewhat arbitrary but is consistent with our SEM analyses of adularia that show $K_2O$ concentrations ≥15.5 percent and undetectable CaO (detection limit = 0.1%; Table 3).

The exceptions to the "high K/Ca" rule are the adularized sanidines, samples H95-51A and D8 271 (Fig. 6). Adularized sanidine in sample H95-51A has abundant calcite inclusions. Calcite appears to have degassed over most of the same temperature range as adularia, so K/Ca ratios were markedly low, ~5 to 35. K/Ca rose to about 400 in the highest temperature steps, suggesting that calcite was nearly completely degassed at these temperatures. Sample D8 271 shows a similar K/Ca pattern, but with generally higher K/Ca values. It does not obviously contain calcite, so a low K/Ca may be, in part, a characteristic of adularized sanidines. SEM analyses showed undetectable CaO, however (Table 3).

Adularia spectra are generally flat, but a few steps are somewhat discordant (e.g., the 1,300°C step in H95-51A; Fig. 6). This irregularity may reflect mixing of gas released from adularia and intergrown alteration minerals or fluid inclusions even in higher temperature steps.

We offer two possible explanations for the aberrant low-temperature fractions. Our preferred interpretation is that gas in these steps was released from a variable mix of adularia, other alteration minerals such as smectite that are not retentive of Ar and are intergrown with adularia, and fluid or vapor inclusions. Smectite and fluid inclusions would degas at low temperatures, much lower than those for adularia. Therefore, Ar release from adularia dominated higher temperature steps. A less likely alternative, of unusual trapped Ar components, is discussed below.

*Isochron analysis*

The plateau age calculation assumes that any trapped, nonradiogenic Ar has an atmospheric composition ($^{40}Ar/^{36}Ar$ = 295.5). Plotting the data on an inverse isochron diagram ($^{36}Ar/^{40}Ar$ vs. $^{39}Ar/^{40}Ar$) allows testing of this assumption (McDou-

gall and Harrison, 1988; Deino and Potts, 1990). Not surprisingly, isochron ages calculated using plateau steps are mostly indistinguishable from the plateau ages and give atmospheric trapped Ar compositions (Table 4). However, in a few cases, isochrons calculated from low-temperature steps, which generally do not reside on the plateau, give different ages and unusual trapped Ar ratios. The best examples are the duplicate analyses of sample HGV (Table 4). Isochron ages from low-temperature steps agree more closely with analyses from the first irradiation and with both plateau and isochron ages from all other samples. The age agreement may simply be fortuitous, because other samples do not show a consistent pattern.

What is more striking is that several samples show trapped Ar components with ratios significantly less than 295.5 (Table 4). This might seem impossible because Ar is not fractionated chemically, and lowering the ratio requires removing $^{40}Ar$ or adding $^{36}Ar$. Possibly a physical process, such as boiling, which has occurred at Round Mountain (Berger, 1985; J. Cline, private report to Round Mountain Gold Corporation, 1992), or diffusion, could fractionate Ar isotopes. In contrast, elevated ratios are easily explained as a result of incorporating radiogenic $^{40}Ar$ from degassing potassium-rich or old rocks. Many examples of trapped Ar with $^{40}Ar/^{36}Ar$ greater than 295.5 are known, including examples of multiple trapped Ar components (Heizler and Harrison, 1988). Fluids in the Valles, New Mexico, hydrothermal system are enriched in $^{40}Ar$ (Musgrave et al., 1994). Enrichment in hydrothermal fluids at Round Mountain, which reacted with the potassium-rich host rhyolites, seems possible, but is not indicated by our data. Further evaluation of the possibility of Ar fractionation by boiling or other processes, although highly speculative, seems warranted, given its implications for hydrothermal processes and dating of ore deposits.

*Reproducibility*

Adularia sample HGV was analyzed three times to test reproducibility, particularly between irradiations at the two reactors. The sample was irradiated once at the University of Michigan and twice, in separate aliquots in a single irradiation package, at Texas A&M University (Table 4). The three analyses agree reasonably well, although data for all nine samples seem to show less scatter than do the replicate analyses. Although all irradiations were closely monitored, irradiations at different reactors with significantly different characteristics offer the greatest possibility for poor reproducibility. For example, the Michigan reactor has a significant radial gradient, which is undetectable at the Texas A&M reactor. However, replicate analyses of sanidine phenocrysts irradiated at the two reactors reproduce within about 0.25 percent (C.D. Henry, unpub. data).

## Duration of Hydrothermal Activity

A combination of field and isotopic data bears on the duration of hydrothermal activity at Round Mountain. Our conclusion is that hydrothermal activity was brief, no more than 0.1 m.y.

*Implications of field relations, $^{40}Ar/^{39}Ar$ ages of volcanic rocks, and sinter*

Dates of approximately 26.5 Ma on the tuff of Round Mountain and of 26.0 Ma on the late or postalteration tuff of Big Smoky Valley limit the duration of hydrothermal activity to no more than 0.5 m.y. and show that it ended no later than 26.0 Ma. Moreover, hydrothermal circulation probably would take a significant amount of time to be established following ash-flow eruption and caldera collapse. Eruption and collapse would generate considerable permeability but would also drain the magma body of most of its silicic component and magmatic volatiles. Even if residual magma remained as a heat source, it probably would lie at depths of at least 5 km, a typical depth for caldera magma chambers (Lipman, 1984), and hydrothermal circulation might take time to be reestablished. Therefore, hydrothermal activity probably started well after 26.5 Ma and lasted much less than 0.5 m.y.

The apparent absence of subaerially or subaqueously deposited sinter in the Stebbins Hill sequence provides somewhat equivocal evidence for a purely late hydrothermal event. We assume that the Stebbins Hill sequence, which was deposited within the closed caldera basin, accumulated progressively between 26.5 and 26.0 Ma, the ages of the underlying and overlying tuffs. No sinter or sinter only in the uppermost parts of this sequence would be consistent with only late hydrothermal activity. Sinter throughout the sequence would indicate more prolonged activity. As noted above, we found no definite sinter in core from the Stebbins Hill sequence. Berger (1985) and Tingley and Berger (1985) reported finely laminated chalcedonic sinter as clasts in what they interpreted to be hydrothermal explosion breccias in the lowermost part of the sequence that formerly capped Round Mountain (Fig. 3). They inferred little vertical transport of breccia clasts, but the top of the sequence, and probably the paleosurface, would have been less than 100 m higher. Sander and Einaudi (1990) argued that the breccias were epiclastic sedimentary deposits and that any sinter was either transported or not related to the ore-forming system. None of these interpretations can be tested now because mining has removed the top of Round Mountain. Sinter, either in place in the uppermost tuff of Round Mountain or in the basal Stebbins Hill sequence or as clasts in sedimentary breccia at these levels, would be puzzling. Sinter in place would require early discharge of hydrothermal fluids, probably close to 26.5 Ma. Sinter as clasts would require an earlier, probably pre-26.5 Ma event and reworking into the caldera basin. Older mineral deposits occur in the Toquima Range (Shawe et al., 1986), but nearby sources of sinter are unknown.

## $^{40}Ar/^{39}Ar$ Ages of Adularia

This discussion uses ages determined by the plateau method (Table 4) because their interpretation is most straightforward. However, using isochron ages would not alter our conclusions. Implications for the duration of hydrothermal activity come from the absolute age range shown by the nine adularia samples, comparison of these ages with the alteration sequence proposed by Sander and Einaudi (1990), and the characteristics of individual age spectra.

*Absolute age range*

Eight adularia ages range from 25.94 ± 0.09 to 26.09 ± 0.08 Ma (the mean of the three analyses of HGV), with one

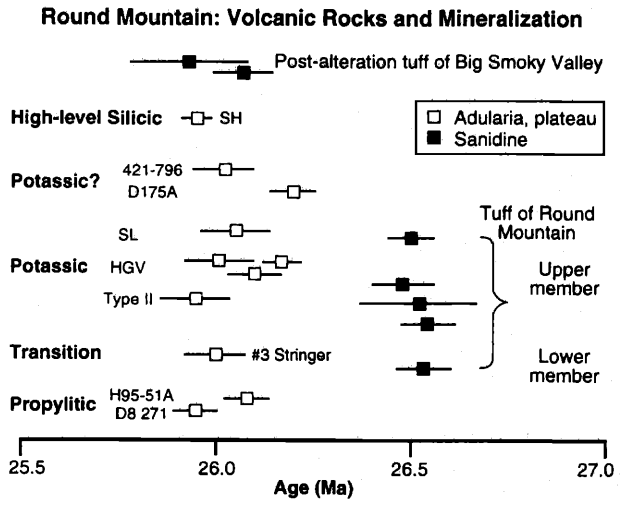


FIG. 7. $^{40}Ar/^{39}Ar$ ages (mean $\pm 1\sigma$) from sanidine of ash-flow tuffs (Table 1 and Henry et al., 1996) and adularia from mineralized rocks at Round Mountain (Table 4). Tuffs are plotted in ascending stratigraphic order; adularia samples are plotted in order of proposed alteration sequence (Sander and Einaudi, 1990), oldest at bottom. Samples 421-796 and D175A probably formed during potassic alteration. Both mean and isochron ages are plotted for the postalteration tuff of Big Smoky Valley. Adularia ages do not correlate with proposed alteration sequence, and variation in ages barely exceeds $\pm 1\sigma$. Variation is probably the result of analytical uncertainty only. Lack of correlation between ages and proposed alteration sequence does not disprove the sequence, only that alteration must have occurred in a time span which is not resolvable even with precise $^{40}Ar/^{39}Ar$ dating.

outlier at 26.20 ± 0.05 (Table 4; Fig. 7). The mean of all nine is 26.03 ± 0.08 Ma. The absolute age range allows a duration of hydrothermal activity of as much as 0.4 m.y., the difference between the high and low ages with their respective $1\sigma$ uncertainties. However, for several reasons, we interpret the spread in ages to reflect analytical uncertainty only and the duration to be much less than 0.4 m.y.

*Comparison with alteration sequence of Sander and Einaudi (1990)*

Dated samples span the proposed alteration sequence of Sander and Einaudi (1990), but the ages do not correlate with it (Table 4; Fig. 7). Most ages overlap within $\pm 1\sigma$. For example, adularization of sanidine is interpreted to have occurred during early propylitic alteration. However, the two samples of adularized sanidine (D8 271 and H95-51A) give one of the oldest and one of the youngest ages; indeed, the two ages cover nearly the entire range of calculated ages. Sample SH, from a coxcomb vein that formed during late, high-level silicic alteration, gives one of the youngest ages but no younger than ages of samples formed during propylitic and potassic alteration. The two samples whose position in the alteration sequence is uncertain also do not support a long duration for alteration. The age of sample 421-796, which may have formed during potassic alteration, falls within the cluster of most ages. Only sample D175A gives an apparent older age. However, it probably also precipitated during potassic alteration, which should place it in the middle of the proposed sequence. Characteristics of its Ar spectrum indicate that adularia in sample D175A did not remain at temperatures of propylitic alteration (~275°C) for an extended period; therefore it probably precipitated at about the same time as all the other samples (see discussion below).

We therefore conclude that the age range reflects analytical uncertainty only. We emphasize that our data do not disprove the alteration sequence of Sander and Einaudi (1990), only that alteration occurred in a time span that is not resolvable even with precise $^{40}Ar/^{39}Ar$ dating.

*Thermal modeling*

Some of the strongest evidence for a brief duration of hydrothermal activity comes from the flatness of individual age spectra. Thermal modeling using the domain characteristics determined for samples H95-51A and D175A (Table 5) does not allow extended periods at 275°C, the maximum temperature inferred from fluid inclusion studies (Sander and Einaudi, 1990).

Figure 8 Illustrates three possible thermal histories and the modeled age spectra they would generate using the diffusion domain characteristics of samples H95-51A and D175A. In all models, adularia precipitates at 26.5 Ma and is maintained at constant temperature until abrupt cooling to 100°C, well below any closure temperature, at 26.0 Ma. The three cases illustrate precipitation at 275°C, the maximum temperature of hydrothermal fluids at Round Mountain (Sander and Einaudi, 1990), 400°C, and 450°C.

For either sample, adularia that precipitated at 275°C would be below closure temperature for most domains but above closure for the least retentive domains. Most domains would retain all radiogenic Ar, whereas some Ar would diffuse out of the least retentive domains. Therefore, Ar released in the lowest temperature steps of the modeled age spectrum would give an age of 26.0 Ma. At higher release temperatures, the apparent age would climb rapidly to 26.5 Ma after about 10 to 20 percent of released $^{39}Ar$. The remaining 80 to 90 percent of the spectrum would be flat at 26.5 Ma, which, in a natural example, would be interpreted as the primary crystallization age. To generate a flat spectrum at 26.0 Ma, adularia that precipitated at 26.5 Ma would have to remain at ≥450°C, well above the closure temperature of all domains (Fig. 8; Table 5). Even at 400°C, the modeled age spectra are not flat. Ar would diffuse out of all but the most retentive domains, which still would not retain all Ar. The 400°C spectra are nearly flat at 26.0 Ma for the first 30 to 40 percent of gas release, then climb to about 26.3 to 26.4 Ma for the final 40 percent of gas release. Low-temperature parts of these spectra indicate the time of final cooling, but higher temperature parts fall below the time of initial crystallization because even the most retentive domains do not retain all Ar.

Modeled age spectra are similar for both samples but reflect the greater proportion of more retentive domains in sample D175A (Fig. 8). Most of the 275°C spectrum for that sample is flat at 26.5 Ma, with only a sharp tail representing at most the first 10 percent of gas released. The 400°C spectrum climbs more steeply in the transition in mid-gas release, and the high-temperature plateau is closer to 26.5 Ma. The 450°C spectrum is distinctly sloped from 26.0 to about 26.2 Ma.

The modeled age spectra demonstrate that adularia which precipitated at 275°C can only have flat spectra if it cooled quickly after formation. The only other way for adularia to have a flat spectrum is for it to precipitate at temperatures

TABLE 5. Kinetic Properties of Adularia

| Sample D175A Activation energy (E) = 55 kcal/mole | | | | Sample H95-51A Activation energy (E) = 53.5 kcal/mole | | | |
|---|---|---|---|---|---|---|---|
| Domain | log(D/r²) | Volume fraction | Closure temperature (°C) | Domain | log(D/r²) | Volume fraction | Closure temperature (°C) |
| 1 | 8.13 | 0.030 | 259 | 1 | 9.04 | 0.025 | 225 |
| 2 | 6.76 | 0.038 | 292 | 2 | 7.94 | 0.054 | 249 |
| 3 | 6.45 | 0.022 | 300 | 3 | 7.22 | 0.057 | 266 |
| 4 | 5.50 | 0.230 | 326 | 4 | 6.45 | 0.090 | 285 |
| 5 | 4.27 | 0.080 | 364 | 5 | 5.40 | 0.146 | 313 |
| 6 | 3.47 | 0.600 | 390 | 6 | 4.75 | 0.070 | 332 |
| | | | | 7 | 3.56 | 0.558 | 370 |

D = Diffusion coefficient
r = characteristic size of diffusion domain

much greater than the closure temperature of the most retentive diffusion domain. Temperatures of 400° to 450°C far exceed those determined from fluid inclusion studies (Sander and Einaudi, 1990). They are also much greater than have been found in any shallow, epithermal system of the adularia-sericite type (Heald et al., 1987). The flat spectra therefore indicate that adularia precipitated and cooled quickly.

The age spectra, geologic data, and alteration sequence of Sander and Einaudi (1990) make any alternative to brief hydrothermal activity unlikely. Two alternative possibilities hinge upon the apparently older age of sample D175A (26.20 ± 0.05 Ma; Table 4; Fig. 6) and require that it be the only dated adularia to have formed at that time. The two possibilities are sustained temperatures of about 275°C between 26.2 and 26.0 Ma or episodic activity, i.e., a 275°C episode at 26.2 Ma, then substantial cooling, then a return to 275°C at 26.0 Ma (Fig. 9).

The age spectrum of sample D175A is inconsistent with sustained 275°C temperatures. If it had precipitated at 26.2 Ma and only cooled at 26.0 Ma, its spectrum would be flat at 26.2 Ma with a low-temperature tail to 26.0 Ma, as in the modeled age spectra (Fig. 8). Instead, low-temperature steps, approximately the first 5 percent of gas release, show greater ages, about 26.5 Ma, even on an inverse isochron plot (Table 4). The origin of these apparent older ages is not certain, but they are inconsistent with prolonged heating.

Two or more episodes of hydrothermal activity are unlikely but cannot be precluded. In this case, sample D175A, which

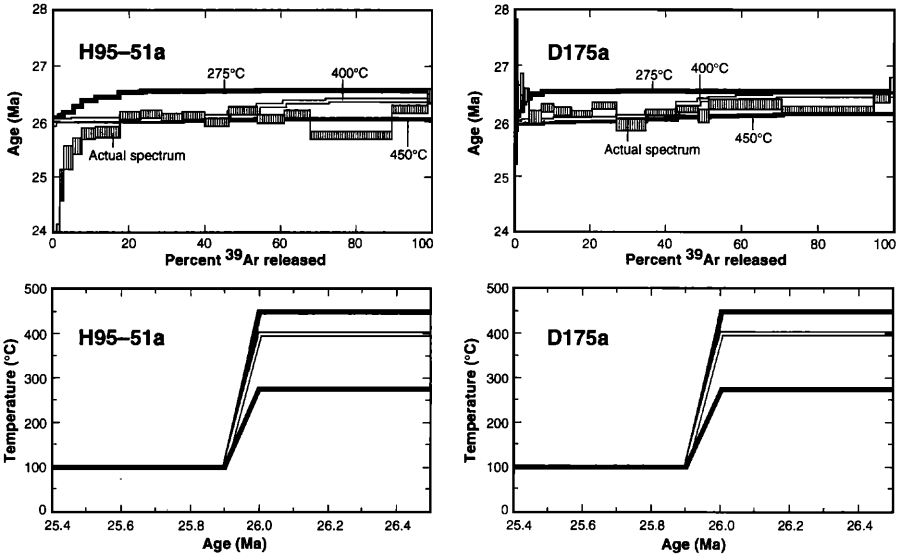


FIG. 8. Actual and modeled age spectra for samples H95-51A and D175A using kinetic properties from Table 5. In all models, adularia is assumed to precipitate at 26.5 Ma and remains at constant temperature until abrupt cooling to 100°C at 26.0 Ma. The three cases illustrate precipitation at 275°C, the maximum temperature of hydrothermal fluids at Round Mountain (Sander and Einaudi, 1990), 400°C, and 450°C. Spectra are similar for both samples but reflect the greater proportion of more retentive domains in sample D175A. For either sample, modeled spectra for adularia that precipitated at 275°C give an age of 26.0 Ma for the lowest temperature steps, then climb rapidly to 26.5 Ma at higher release temperatures. The remaining 80 to 90 percent of the spectra are flat at 26.5 Ma, which, in a natural example, would be interpreted as the primary crystallization age. To generate a flat spectrum at 26.0 Ma, adularia that precipitated at 26.5 Ma would have to remain at ≥450°C, well above the closure temperature of all domains and hydrothermal temperatures at Round Mountain. Therefore, the flat spectra of all samples (Fig. 6) require that they precipitate and cool rapidly. Lower boxes show modeled cooling histories of the samples.

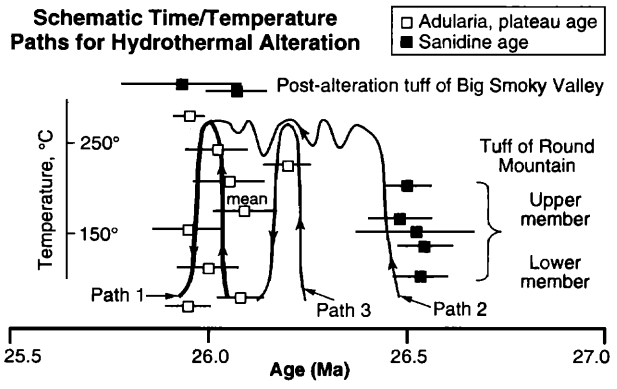


FIG. 9. Schematic, alternative time-temperature paths during hydrothermal alteration at Round Mountain. Ages are plotted in order of proposed alteration sequence, as in Figure 7, except that "mean" shows the mean and standard deviation of three analyses of sample HGV. Temperature scale at left is for possible hydrothermal temperature paths 1, 2, and 3. Alteration was most likely a geologically brief event, no more than approximately 0.1 m.y. long, that occurred at about 26.0 Ma (path 1). Flatness of Ar release spectra from individual adularia samples precludes sustained (>0.1 m.y.) high temperatures similar to those of propylitic alteration (275°C; path 2). An early episode of alteration (path 3), followed by cooling, and then a second episode (path 1) cannot be disproven but is unlikely. By any path, date on late tuff confirms that hydrothermal alteration ended at approximately 26.0 Ma. See text for discussion.

most likely formed during potassic alteration, would have precipitated and cooled at 26.2 Ma and be the only dated sample from this first episode (Fig. 9). All other dated adularia, including the two adularized sanidine phenocrysts from propylitic alteration, would have to have formed during a second episode at 26.0 Ma. This interpretation is inconsistent with the temporal alteration interpretation of Sander and Einaudi (1990). That is, once potassic alteration began, conditions of propylitic alteration never returned. Early formation of sample D175A is also inconsistent with a spatial view of alteration as a potassic core with a propylitic halo. Sample D175A formed in the same volume of rock as other samples and therefore should have undergone the same thermal history. Also, although we are uncertain what the spectra of adularia that underwent such a cyclic process would look like, nothing in the D175A spectrum indicates an unusual history. Episodic alteration requires a complex thermal history that is not supported by any of our age data or by the petrographic data of Sander and Einaudi (1990). We conclude, therefore, that the slightly greater age of D175A reflects analytical uncertainty only, as was concluded for the complete range of ages.

A third alternative, of 275°C temperatures being sustained after 26.0 Ma, is suggested by the spectra of samples H95-51A and D8 271 (Figs. 6 and 8). These spectra are similar to the modeled 275°C spectrum (Fig. 8). That is, the lowest temperature steps show ages below 26.0 Ma, but 80 to 90 percent of the spectra plateau at 26.0 Ma. This pattern could be interpreted to indicate that temperatures of 275°C were maintained well after 26.0 Ma so that the least retentive domains lost some Ar. However, the 26.0 Ma age of the tuff of Big Smoky Valley demonstrates that hydrothermal activity ceased at that time. As discussed above, these low-temperature steps most likely indicate degassing of nonretentive phases that form inclusions in adularia.

## Discussion

Brief duration of hydrothermal activity at Round Mountain is supported by consideration of the mechanism of Au deposition, by comparison with some modern geothermal systems, and by the likely life span of magmatic systems. First, from solubility constraints on Au, fluid-mineral equilibria, and reasonable fluid-rock ratios, Sander and Einaudi (1990) concluded that all gold at Round Mountain could be deposited in approximately 0.1 m.y.

Second, Hedenquist and Henley (1985) estimated that the active geothermal system at Waiotapu, New Zealand, has precipitated approximately 100,000 oz of Au beneath one hydrothermal vent in as little as 900 years. They argue that gold deposits of the size of Round Mountain could form in as little as 10,000 years, a possibility that cannot be eliminated by our data.

Finally, the duration of hydrothermal convection is a function of the life span of its heat source. Without replenishment, even caldera-sized silicic magma bodies cool and solidify in no more than about 100,000 years (Lachenbruch et al., 1976; Spera, 1979; Cathles, 1981; Halliday et al., 1989). Although the hot intrusion remains as a heat source after solidification, hydrothermal convection only increases heat loss and cooling (Lachenbruch et al., 1976; Cathles, 1981). Hydrothermal systems related to calderas can survive no more than a few hundred thousand years unless the heat source is replenished (Lachenbruch et al., 1976; Cathles, 1981). We interpret the Round Mountain system to have been driven by a concealed ring fracture intrusion (see below and Henry et al., 1996), much smaller than the overall caldera magma body, so the duration of its hydrothermal system would have been still less.

Our conclusion of brief activity at Round Mountain contrasts with a common interpretation that hydrothermal systems, even shallow epithermal systems, are long-lived, with life times of up to several million years (Silberman et al., 1979; Whalen et al., 1982; Silberman, 1985; Criss et al., 1991; Conrad et al., 1993). This is less of a contradiction than it first appears. Long-lived commonly means several episodes of hydrothermal activity over an extended period (Silberman et al., 1979; Silberman, 1985; Conrad et al., 1993). Most notably, the apparent 3-m.y. duration of activity at Steamboat Springs, Nevada, reflects at least three episodes of hydrothermal alteration (and probably of magmatism) at about 3 m.y., 1.1 m.y., and the present, not continuous activity (Silberman et al., 1979).

Moreover, evidence of long-lived hydrothermal activity is lacking in most systems, particularly shallow ones. Most studies are based upon K-Ar dating of Tertiary igneous rocks and ore deposits. K-Ar dating does not have the resolution to distinguish a 0.1-m.y. episode from a 1.0-m.y. episode in mid-Tertiary rocks. For example, previous K-Ar dates of the host tuff and alteration minerals at Round Mountain range from 24.4 to 27.3 and 25.4 to 26.6 Ma, respectively (Table 6). The mean of 11 K-Ar ages on biotite and sanidine of the tuff of Round Mountain is 26.4 ± 0.9 Ma; the mean of six adularia and one sericite ages is 25.9 ± 0.5 (Table 6). The mean

TABLE 6. Previous K-Ar Dates at Round Mountain

| Sample number or unit | Material | Age (Ma) | ±1σ | Reference |
|---|---|---|---|---|
| Mineralization | | | | |
| Coxcomb vein, Stebbins Hill | Adularia | 26.5 | 0.6 | Sander (1988) |
| Adularized sanidine | Adularia | 26.6 | 0.6 | Sander (1988) |
| Partly adularized sanidine | Adularia-sanidine | 25.8 | 0.5 | Sander (1988) |
| Partly adularized sanidine | Adularia-sanidine | 25.7 | 0.6 | Sander (1988) |
| DRS 146-68 | Adularia | 25.9 | 0.8 | Shawe et al. (1986) |
| Mariposa vein | Sericite | 25.4 | 0.8 | Tingley and Berger (1985) |
| Mariposa vein[1] | Alkali feldspar | 25.5 | 0.8 | Tingley and Berger (1985) |
| Mean | | 25.9 | 0.5 | |
| Tuff of Round Mountain (all upper member of this report) | | | | |
| Ting-81-1 | Sanidine | 25.7 | 0.7 | Tingley and Berger (1985) |
| DRS-79-85 | Biotite | 26.7 | 1.7 | Shawe et al. (1987) |
| DRS-79-85 | Sanidine | 26.8 | 1.0 | Shawe et al. (1987) |
| RM 1 | Sanidine | 26.8 | 0.8 | Silberman et al. (1975) |
| 723-SP-S | Sanidine | 26.5 | 0.4 | Boden (1992) |
| 723-SP-B | Biotite | 27.2 | 0.6 | Boden (1992) |
| 720-SP-S | Sanidine | 26.8 | 0.6 | Boden (1992) |
| 720-SP-B | Biotite | 25.5 | 0.6 | Boden (1992) |
| 217-SP | Sanidine | 27.3 | 1.1 | Boden (1992) |
| K-Ar-RM-2 | Sanidine | 26.8 | 0.5 | Boden (1992) |
| K-Ar-RM-2 | Biotite | 24.4 | 0.6 | Boden (1992) |
| Mean | | 26.4 | 0.9 | |

[1] Interpreted to be an alteration age, but may date host tuff

values agree well with our means of 26.51 ± 0.03 Ma on five sanidines (Table 1) and of 26.03 ± 0.08 Ma on nine adularia (Table 4). The K-Ar data reveal the general timing of magmatism and mineralization and that the two were generally contemporaneous. However, neither individual K-Ar ages nor averages of many ages resolved the duration of hydrothermal activity nor the time gap between tuff emplacement and hydrothermal activity. Furthermore, our most precise constraint from $^{40}Ar/^{39}Ar$ dating on the duration of activity comes from the ability of age spectra to decipher complex thermal history beyond simply providing an age.

*What drove the Round Mountain hydrothermal system?*

We support the interpretation of Berger et al. (1986) that the hydrothermal activity at Round Mountain was driven by a concealed intrusion emplaced along the ring fracture. This interpretation is consistent with the geologic and geochronologic data on Round Mountain and is supported by comparisons with other calderas and ore deposits. The most critical evidence is that the deposit directly overlies the ring fracture of the Round Mountain caldera (Figs. 2 and 3), which formed just 0.5 m.y. before ore deposition.

Ring fracture intrusions and lava domes are nearly ubiquitous features of caldera magmatism (Smith and Bailey, 1968; Lipman, 1984). Calderas and other large magmatic systems are typically active, episodically, for 1 m.y. or more. Detailed studies of the three large, young calderas of the western United States (Long Valley, California; Yellowstone National Park; and Valles, New Mexico) show that ring fracture intrusion and volcanism occurred in brief episodes separated by repose times of several hundred thousand years (Bailey et al., 1976; Hildreth et al., 1984; Spell and Harrison, 1993, respectively). Numerous silicic domes lie along the ring fractures of the Mount Jefferson and Moores Creek calderas in the adjacent Toquima Range (Boden, 1986, 1992). These domes were emplaced in distinct episodes several hundred thousand years after ash-flow eruption and caldera collapse (C.D. Henry, unpub. $^{40}Ar/^{39}Ar$ data). It would be surprising if late ring fracture intrusions were absent from the Round Mountain caldera.

Adularia-sericite deposits generally are interpreted to be driven by shallow intrusions that are distant from the deposit (Heald et al., 1987; Sillitoe, 1989). The geologic setting of the deposit at Creede, Colorado, in the San Juan caldera complex, is similar to that of Round Mountain. Creede lies near the intersection of three or four calderas, and hydrothermal circulation is interpreted to have been driven by a silicic stock directly beneath the district at a depth of 3 to 5 km and is probably related to the youngest caldera (Steven and Eaton, 1975; Bethke and Lipman, 1987; Lipman, 1992).

The location and depth of the postulated intrusion at Round Mountain is unknown. Numerous dikes, sills, and other small intrusions have been encountered by drilling. However, most of these are petrographically similar to the 34 to 37 Ma intrusions exposed to the east in the Toquima Range (Fig. 2) and are too small to constitute a significant heat source. Nevertheless, some could be apophyses from the postulated body. Because adularia-sericite deposits may be far from their heat source (Heald et al., 1987; Sillitoe, 1989), the postulated intrusion at Round Mountain could be several kilometers away; mineralization was localized by favorable ring-fault structure, host rock, and paleohydrology.

This postulated ring fracture intrusion cannot simply be an apophysis from the early caldera magma body. Without additional input of magma and heat from another source, even the presumably 11-km-diameter caldera magma body

would have cooled to the point where it was not a viable heat source in 0.5 m.y. (Lachenbruch et al., 1976; Cathles, 1981). The similarity in age between adularia and the tuff of Big Smoky Valley allows the possibility that both hydrothermal circulation and the tuff are related to a late phase of the caldera magma system.

The close temporal association between the Round Mountain deposit and host rock is apparently unusual for adularia-sericite systems where ore deposition generally postdates host-rock formation by more than 1 m.y. (Heald et al., 1987). Heald et al, citing previous K-Ar dates, noted that Round Mountain is an exception. We suggest that exceptions may be more common. First, we reemphasize the inability of conventional K-Ar dating to resolve small age differences. Dating minerals formed during hydrothermal alteration can be particularly difficult. Also, many adularia-sericite deposits formed in nested caldera complexes, such as the San Juan Mountains, where igneous activity occurred over several million years. In such settings, deposits may reside in older igneous rocks but be related to a contemporaneous caldera (Lipman et al., 1976). Mineral deposits at Creede, Colorado, illustrate this point. Ore occupies faults cutting older caldera-fill ash-flow tuff, but hydrothermal activity probably is related to the youngest caldera (Steven and Eaton, 1975; Bethke and Lipman, 1987). Adularia-sericite deposits may occupy older host rocks simply because they commonly are distal to the heat source.

### *Depth of mineralization*

Depth of mineralization at Round Mountain is controversial. Berger (1985) cited Round Mountain as a typical example of a hot spring precious metal deposit that formed essentially at the paleosurface. For example, the clasts of sinter found by Tingley and Berger (1985) would indicate a paleodepth to the top of the tuff of Round Mountain at the time of mineralization of no more than about 10 m. In contrast, Sander and Einaudi (1990) calculated a minimum paleodepth to the top of the tuff of Round Mountain of about 400 m. This depth is based on maximum fluid inclusion homogenization temperatures of 275°C within the upper member of the tuff of Round Mountain and assumed hydrodynamic pressures (Henley, 1985). Additional fluid inclusion data generally support their temperature determinations and document boiling (Berger, 1985; J.S. Cline, private report to Round Mountain Gold Corporation, 1992).

Our geologic and geochronologic data suggest a paleodepth of 100 m to the top of the tuff of Round Mountain. This value is based on the observation that the entire 90-m-thick Stebbins Hill sequence is hydrothermally altered and on our interpretation that the top of the sequence was probably the paleosurface at the time of mineralization. The Stebbins Hill sequence was deposited within what must have been a closed caldera basin, so erosion to strip off overlying, altered rocks is unlikely. Also, the $^{40}Ar/^{39}Ar$ age of the tuff of Big Smoky Valley is indistinguishable from adularia ages (Tables 1, 4; Fig. 7). The tuff must have been deposited on the paleosurface either immediately following mineralization or at the very end of the system, giving little time for either erosion or deposition. By this interpretation, ore formed within the upper part of the Stebbins Hill sequence at paleodepths of only a few tens of meters.

We offer the following possible reconciliations for these different estimates; none is fully satisfactory:

1. Pressures locally exceeded hydrodynamic because intense silicification created an impermeable cap, leading to hydrothermal brecciation (e.g., Berger, 1985). Pressures reaching or exceeding lithostatic have been called upon in other hydrothermal systems (Hedenquist and Henley, 1985), but Sander and Einaudi (1990) considered such conditions to be rare.
2. A deep lake covered the area accounting for high hydrodynamic pressures despite little rock cover. The Stebbins Hill sequence accumulated within a closed caldera basin and includes probable lake deposits, so a lake was present at least part of the time. However, some Stebbins Hill rocks appear to be subaerial deposits, and the tuff of Big Smoky Valley definitely is subaerial. Any lake would have to have drained abruptly between the end of hydrothermal activity and deposition of the tuff.
3. Additional sedimentary rocks overlay the preserved Stebbins Hill sequence at the time of alteration but were stripped following alteration and before deposition of the tuff of Big Smoky Valley. This would require that approximately 300 m of rock be eroded from within a closed basin in probably much less than 100,000 years.
4. The tuff of Big Smoky Valley was deposited before alteration but was impermeable to hydrothermal fluids and so is only weakly altered at its nonwelded base. This weak alteration suggests that the tuff was emplaced at the very end of the hydrothermal system (D.R. Boden, pers. commun., 1995). Impermeability of only the densely welded part seems unlikely to have prevented more extensive alteration because the equally densely welded upper member of the tuff of Round Mountain is intensely altered and veined. Therefore, the tuff of Big Smoky Valley was probably not in place during most of the period of alteration.

## Summary

The Round Mountain gold-silver deposit is intimately associated with caldera magmatism and structure and strengthens the general association of adularia-sericite deposits with calderas (Heald et al., 1987; Lipman, 1992). The deposit overlies the ring fracture of the Round Mountain caldera, which collapsed during eruption of the tuff of Round Mountain (Henry et al., 1996). The tuff erupted in two pulses, a lower member that is more than 600 m thick and an upper member that is as much as 390 m thick. $^{40}Ar/^{39}Ar$ ages of sanidine from the two members are indistinguishable; five analyses give a mean age of 26.51 ± 0.02 Ma. Following ash-flow eruption and caldera collapse, about 90 m of lake beds, debris deposits, and minor pyroclastic-fall and ash-flow tuff (the Stebbins Hill sequence) accumulated within the caldera basin. All of these rocks are hydrothermally altered and contain ore. The late- or postalteration tuff of Big Smoky Valley overlies mineralized rock and dates at 26.0 Ma, which places a 0.5-m.y. upper limit on the duration of hydrothermal activity.

$^{40}Ar/^{39}Ar$ ages of adularia indicate that hydrothermal convection was a brief event, no more than about 0.1 m.y. long,

at about 26.0 Ma. Ages were determined on nine adularia samples that formed throughout the deposit and span the proposed temporal alteration sequence of Sander and Einaudi (1990). The mean of the nine ages is 26.03 ± 0.08 Ma. Comparison of adularia age spectra with modeled spectra determined from adularia closure temperatures provides the tightest constraint on the duration of hyrothermal activity. Flat age spectra indicate that the duration may have been as little as 50,000 years, the uncertainty in individual ages. The data preclude sustained (>0.1 m.y.) temperatures of 275°C, the maximum determined from fluid inclusions. If the alteration history of Sander and Einaudi (1990) is correct, then most Au deposition occurred during an even more limited time during the transition from propylitic to potassic alteration.

The timing of hydrothermal activity and its location along the caldera ring fracture suggest that convective fluid flow was driven by a concealed silicic intrusion. The intrusion was probably emplaced along the ring fracture, but its location and depth are uncertain. Comparison with other adularia-sericite deposits indicates that the intrusion could be several kilometers from the deposit. The hiatus of ~0.5 m.y. between eruption of the tuff of Round Mountain and hydrothermal activity indicates that activity was not simply related to the original caldera magma body, which would not have been a viable heat source after cooling for that length of time.

## Acknowledgments

We thank Dave Boden, Jean Cline, Larry Garside, Larry McMaster, Ralph Mulhollen, Craig Pickens, Mark Sander, Dan Shawe, Jeff Spence, Joe Tingley, Bruce Veek, and Danny Zampirro for discussions about the geology and mineralization of the Toquima Range and Round Mountain; Rich Esser for knowledgable and patient assistance in the exceptional $^{40}Ar/^{39}Ar$ laboratory at the New Mexico Bureau of Mines and Mineral Resources; and three *Economic Geology* referees for thorough, constructive reviews.

## REFERENCES

Bailey, R.A., Dalrymple, G.B., and Lanphere, M.A., 1976, Volcanism, structure, and geochronology of Long Valley caldera, Mono County, California: Journal of Geophysical Research, v. 81, p. 725–744.

Berger, B.R., 1985, Hot spring type gold deposits: U.S. Geological Survey Bulletin 1646, p. 47–53.

Berger, B.R., and Silberman, M.L., 1985, Relationships of trace-element patterns to geology in hot spring-type precious metal deposits: Reviews in Economic Geology, v. 2, p. 233–247.

Berger, B.R., Tingley, J.V., Harrington, R.J., and Grimes, D.J., 1986, Geochemistry of volcanic rocks, Round Mountain mining district, Nevada: Nevada Bureau of Mines and Geology Report 41, p. 131–134.

Best, M.G., Christiansen, E.H., Deino, A.L., Gromme, C.S., McKee, E.H., and Noble, D.C., 1989, Eocene through Miocene volcanism in the Great Basin of the western United States: New Mexico Bureau of Mines and Mineral Resources Memoir 47, p. 91–133.

Bethke, P.M., and Lipman, P.W., 1987, Deep environment of volcanogenic epithermal mineralization—proposed research drilling at Creede, Colorado: EOS, v. 68, p. 187–189.

Boden, D.R., 1986, Eruptive history and structural development of the Toquima caldera complex, central Nevada: Geological Society of America Bulletin, v. 97, p. 61–74.

——1992, Geologic map of the Toquima caldera complex, central Nevada: Nevada Bureau of Mines and Geology Map 98, scale 1:48,000.

Bonham, H.F., Jr., and Hess, R.H., 1995, Major precious-metal deposits: Nevada Bureau of Mines and Geology Special Publication MI-1994, p. 23–35.

Brem, G.F., and Snyder, D.B., 1983, Lithologic and gravity characteristics of the southern Peavine volcanic center, Toiyabe Range, Nevada: Geological Society of America Abstracts with Programs, v. 15, p. 280.

Brem, G.F., John, D.A., Nash, J.T., Poole, F.G., and Snyder, D.B., 1991, Mineral resources of the Arc Dome wilderness recommendation area, Nye County, Nevada: U.S. Geological Survey Bulletin 1961, 21 p.

Burgess, R., and Parsons, I., 1994, Argon and halogen geochemistry of hydrothermal fluids in the Lock Ainort granite, Isle of Skye, Scotland: Contributions to Mineralogy and Petrology, v. 115, p. 345–355.

Burgess, R., Kelley, S.P., Parsons, I., Walker, F.D.L., and Worden, R.H., 1992, $^{40}Ar$-$^{39}Ar$ analysis of perthite microstructures and fluid inclusions in alkali feldspars from the Klokken syenite, South Greenland: Earth and Planetary Science Letters, v. 109, p. 147–167.

Cathles, L.M., 1981, Fluid flow and genesis of hydrothermal ore deposits: Economic Geology 75th Anniversary Volume, p. 424–457.

Cebula, G.T., Kunk, M.J., Mehnert, H.H., Naeser, C.W., Obradovich, J.D., and Sutter, J.F., 1986, The Fish Canyon Tuff, a potential standard for the $^{40}Ar/^{39}Ar$ and fission-track dating methods [abs.]: Terra Cognita, v. 6, p. 139–140.

Conrad, J.E., McKee, E.H., Rytuba, J.J., Nash, J.T., and Utterback, W.C., 1993, Geochronology of the Sleeper deposit, Humboldt County, Nevada: Epithermal gold-silver mineralization following emplacement of a silicic flow-dome complex: Economic Geology, v. 88, p. 317–327.

Criss, R.E., Fleck, R.J., and Taylor, H.P., Jr., 1991, Tertiary meteoric hydrothermal systems and their relations to ore deposition, northwestern United States and southern British Columbia: Journal of Geophysical Research, v. 96, p. 13,335–13,356.

Deino, A., and Potts, R., 1990, Single-crystal $^{40}Ar/^{39}Ar$ dating of the Olorgesailie Formation, southern Kenya rift: Journal of Geophysical Research, v. 95, p. 8453–8470.

Dodson, M.H., 1973, Closure temperature in cooling geochronological and petrological systems: Contributions to Mineralogy and Petrology, v. 40, p. 259–274.

Ferguson, H.G., 1921, The Round Mountain district, Nevada: U.S. Geological Survey Bulletin 725-I, p. 383–406.

Ferguson, H.G., and Cathcart, S.H., 1924, Geology of the Round Mountain quadrangle, Nevada: U.S. Geological Survey Geological Quadrangle Map GQ-49, scale 1:125,000.

FitzGerald, J.D., and Harrison, T.M., 1993, Argon diffusion domains in K-feldspar I: Microstructures in MH-10: Contributions to Mineralogy and Petrology, v. 113, p. 367–380.

Fleck, R.J., Sutter, J.F., and Elliott, D.H., 1977, Interpretation of discordant $^{40}Ar/^{39}Ar$ age-spectra of Mesozoic tholeiites from Antarctica: Geochimica et Cosmochimica Acta, v. 41, p. 15–32.

Foland, K.A., 1994, Argon diffusion in feldspars, *in* Parsons, I., ed., Feldspars and their reactions: Boston, Kluwer Academic Pub., p. 415–447.

Halliday, A.N., Mahood, G.A., Holden, P., Metz, J.M., Dempster, T.J., and Davidson, J.P., 1989, Evidence for long residence times of rhyolitic magma in the Long Valley magmatic system: The isotopic record in precaldera lavas of Glass Mountain: Earth and Planetary Science Letters, v. 94, p. 274–290.

Harrington, K.J., 1985, Geology and geochemistry of the Mt. Jefferson caldera complex, Nye County, Nevada: Unpublished M.S. thesis, Boulder, University of Colorado, 75 p.

Harrison, T.M., Heizler, M.T., and Lovera, O.M., 1993, In vacuo crushing experiments and K-feldspar thermochronometry: Earth and Planetary Science Letters, v. 117, p. 169–180.

Harrison, T.M., Heizler, M.T., Lovera, O.M., Chen, W., and Grove, M., 1994, A chlorine disinfectant for excess argon released from K-feldspar during step heating: Earth and Planetary Science Letters, v. 123, p. 95–104.

Heald, P., Foley, N.K., and Hayba, D.O., 1987, Comparative anatomy of volcanic-hosted epithermal deposits: Acid-sulfate and adularia-sericite types: Economic Geology, v. 82, p. 1–26.

Hedenquist, J.W., and Henley, R.W., 1985, Hydrothermal eruptions in the Waiotapu geothermal system, New Zealand: Their origin, associated breccias, and relation to precious metal mineralization: Economic Geology, v. 80, p. 1640–1668.

Heizler, M.T., and Harrison, T.M., 1988, Multiple trapped argon isotope components revealed by $^{40}Ar/^{39}Ar$ isochron analysis: Geochimica et Cosmochimica Acta, v. 52, p. 1295–1303.

——1992, K-feldspar $^{40}Ar/^{39}Ar$ constraints on the thermal evolution of New York [abs.]: EOS, v. 73, p. 653.

Heizler, M.T., Lux, D.R., and Decker, E.R., 1988, The age and cooling history of the Chain of Ponds and Big Island Pond plutons and the Spider Lake granite, west-central Maine and Quebec: American Journal of Science, v. 288, p. 925–952.

Henley, R.W., 1985, The geothermal framework for epithermal deposits: Reviews in Economic Geology, v. 2, p. 1–24.

Henry, C.D., Castor, S.B., and Elson, H.B., 1996, Geology and $^{40}Ar/^{39}Ar$ geochronology of volcanism and mineralization at Round Mountain, Nevada, *in* Coyner, A.R., and Fahey, P.L., eds., Geology and ore deposits of the American Cordillera. Symposium Proceedings: Reno/Sparks, Geological Society of Nevada, p. 283–307.

Hildreth, W., Christiansen, R.L., and O'Neil, J.R., 1984, Catastrophic isotopic modification of rhyolitic magma at times of caldera subsidence, Yellowstone Plateau volcanic field: Journal of Geophysical Research, v. 89, p. 8339–8369.

John, D.A., 1992, Stratigraphy, regional distribution, and reconnaissance geochemistry of Oligocene and Miocene volcanic rocks in the Paradise Range and northern Pactolus Hills, Nye County, Nevada: U.S. Geological Survey Bulletin 1974, 67 p.

Kleinhampl, F.J., and Ziony, J.I., 1985, Geology of northern Nye County, Nevada: Nevada Bureau of Mines and Geology Bulletin 99A, 172 p.

Lachenbruch, A.H., Sorey, M.I., Lewis, R.E., and Sass, J.H., 1976, The near-surface hydrothermal regime of Long Valley caldera: Journal of Geophysical Research, v. 81, p. 763–784.

Lee, J., 1995, Rapid uplift and rotation of mylonitic rocks from beneath a detachment fault: Insights from potassium feldspar $^{40}Ar/^{39}Ar$ thermochronology, northern Snake Range, Nevada: Tectonics, v. 14, p. 54–77.

Leloup, P.H., Harrison, T.M., Ryerson, F.J., Chen., W., Li, Q., Tapponnier, P., and Lacassin, R., 1992, Structural, petrological and thermal evolution of a Tertiary ductile strike-slip shear zone, Diancang Shan, Yunnan: Journal of Geophysical Research, v. 98, p. 6713–6744.

Lipman, P.W., 1984, The roots of ash flow calderas in western North America: Windows into the tops of granitic batholiths: Journal of Geophysical Research, v. 89, p. 8801–8841.

——1992, Ash-flow calderas as structural controls of ore deposits—recent work and future problems: U.S. Geological Survey Bulletin 2012, p. L1-L12.

Lipman, P.W., Fisher, F.S., Mehnert, H.H., Naeser, C.W., Luedke, R.G., and Steven, T.A., 1976, Multiple ages of mid-Tertiary mineralization and alteration in the western San Juan Mountains, Colorado: ECONOMIC GEOLOGY, v. 71, p. 571–588.

Lovera, O.M., Heizler, M.T., and Harrison, T.M., 1993, Argon diffusion domains in K-feldspar II: Kinetic properties of MH-10 K-feldspar: Contributions to Mineralogy and Petrology, v. 113, p. 381–393.

Lovera, O.M., Richter, F.M., and Harrison, T.M., 1989, The $^{40}Ar/^{39}Ar$ thermochronology for slowly cooled samples having a distribution of diffusion domain sizes: Journal of Geophysical Research, v. 94, p. 17,917–17,935.

——1991, Diffusion domains determined by $^{39}Ar$ releases during step heating: Journal of Geophysical Research, v. 96, p. 2057–2069.

McDougall, I., and Harrison, T.M., 1988, Geochronology and thermochronology by the $^{40}Ar/^{39}Ar$ method: New York, Oxford University Press, 212 p.

McKee, E.H., 1974, Northumberland caldera and Northumberland Tuff: Nevada Bureau of Mines and Geology Report 19, p. 35–41.

——1976, Geology of the northern part of the Toquima Range, Lander, Eureka, and Nye Counties, Nevada: U.S. Geological Survey Professional Paper 931, 49 p.

Mills, B.A., 1984, Geology of the Round Mountain gold deposit, Nye County, Nevada: Arizona Geological Society Digest, v. 15, p. 89–99.

Mills, B.A., Boden, D.R., and Sander, M.V., 1988, Alteration and precious metal mineralization associated with the Toquima caldera complex, Nye County, Nevada, *in* Schafer, R.W., Cooper, J.J., and Vikre, P.G., eds., Bulk mineable precious metals deposits of the western United States. Symposium Proceedings: Reno, Geological Society of Nevada, p. 303–332.

Musgrave, J.A., Poths, J., and Norman, D.I., 1994, Fluid inclusion noble gas geochemistry of hydrothermal systems in the Rio Grande rift [abs.]: Geological Society of America Abstracts with Programs, v. 26, p. A-356.

Parsons, I., Rex, D.C., Guise, P., and Haliday, A.N., 1988, Argon-loss by alkali feldspars: Geochimica et Cosmochimica Acta, v. 52, p. 1097–1112.

Plouff, D., 1992, Bouguer gravity anomaly and isostatic residual gravity maps of the Tonopah 1° by 2° quadrangle, central Nevada: U.S. Geological Survey Miscellaneous Field Studies Map MF-1877-D, 1:250,000.

Ransome, F.L., 1909, Round Mountain, Nevada: U.S. Geological Survey Bulletin 380, p. 44–47.

Samson, S.D., and Alexander, E.C., Jr., 1987, Calibration of the interlaboratory $^{40}Ar/^{39}Ar$ dating standard, MMhb-1: Chemical Geology, v. 66, p. 27–34.

Sander, M.V., 1988, Epithermal gold-silver mineralization, wall-rock alteration, and geochemical evolution of hydrothermal fluids in the ash-flow tuff at Round Mountain, Nevada: Unpublished Ph.D. dissertation, Stanford University, 283 p.

Sander, M.V., and Einaudi, M.T., 1990, Epithermal deposition of gold during transition from propylitic to potassic alteration at Round Mountain, Nevada: ECONOMIC GEOLOGY, v. 85, p. 285–311.

Shawe, D.R., 1986, Stratigraphic nomenclature of volcanic rocks near Manhattan, southern Toquima Range, Nye County, Nevada: U.S. Geological Survey Bulletin 1775-A, p. A1-A8.

——1995, Geologic map of the Round Mountain quadrangle, Nye County, Nevada: U.S. Geological Survey Geologic Quadrangle Map GQ-1756, 1:24,000.

Shawe, D.R., and Snyder, D.B., 1988, Ash-flow eruptive megabreccias of the Manhattan and Mount Jefferson calderas, Nye County, Nevada: U.S. Geological Survey Professional Paper 1471, 28 p.

Shawe, D.R., Marvin, R.F., Andriessen, P.A.M., Mehnert, H.H., and Merritt, V.M., 1986, Ages of igneous and hydrothermal events in the Round Mountain and Manhattan gold districts, Nye County, Nevada: ECONOMIC GEOLOGY, v. 81, p. 388–407.

Shawe, D.R., Naeser, C.W., Marvin, R.F., and Mehnert, H.H., 1987, New radiometric ages of igneous and mineralized rocks, southern Toquima Range, Nye County, Nevada: Isochron/West, no. 50, p. 3–7.

Silberman, M.L., 1985, Geochronology of hydrothermal alteration and mineralization; Tertiary epithermal precious-metal deposits in the Great Basin: U.S. Geological Survey Bulletin 1646, p. 55–70.

Silberman, M.L., and Berger, B.R., 1985, Relationships of trace-element patterns to alteration and morphology in epithermal precious metal deposits: Reviews in Economic Geology, v. 2, p. 203–232.

Silberman, M.L., White, D.E., Keith, T.E.C., and Dockter, R.D., 1979, Duration of hydrothermal activity at Steamboat Springs, Nevada, from ages of spatially associated volcanic rocks: U.S. Geological Survey Professional Paper 458-D, 14 p.

Sillitoe, R.H., 1989, Gold deposits in western Pacific island arcs: The magmatic connection: ECONOMIC GEOLOGY MONOGRAPH 6, p. 274–291.

Smith, R.L., and Bailey, R.A., 1968, Resurgent cauldrons: Geological Society of America Memoir 116, p. 613–662.

Snyder, D.B., and Healey, D.L., 1983, Interpretation of the Bouguer gravity map of Nevada: Tonopah sheet: Nevada Bureau of Mines and Geology Report 38, 14 p.

Spell, T.L., and Harrison, T.M., 1993, $^{40}Ar/^{39}Ar$ geochronology of post-Valles caldera rhyolites, Jemez volcanic field, New Mexico: Journal of Geophysical Research, v. 98, p. 8031–8051.

Spera, F.J., 1979, Thermal evolution of plutons: A parameterized approach: Science, v. 297, p. 299–301.

Steiger, R.H., and Jager, E., 1977, Subcommission on geochronology: Convention on the use of decay constants in geo- and cosmochronology: Earth and Planetary Science Letters, v. 36, p. 359–362.

Steven, T.A., and Eaton, G.P., 1975, Environment of ore deposition in the Creede mining district, San Juan Mountains, Colorado: I. Geologic, hydrologic, and geophysical setting: ECONOMIC GEOLOGY, v. 70, p. 1023–1037.

Stewart, J.H., and Carlson, J.E., 1978, Geologic map of Nevada: U.S. Geological Survey, scale 1:500,000.

Tingley, J.V., and Berger, B.R., 1985, Lode gold deposits of Round Mountain, Nevada: Nevada Bureau of Mines and Geology Bulletin 100, 62 p.

Turner, G., and Wang, S., 1992, Excess argon, crustal fluids and apparent isochrons from crushing K-feldspar: Earth and Planetary Science Letters, v. 110, p. 193–211.

Whalen, J.B., Britten, R.M., and McDougall, I., 1982, Geochronology and geochemistry of the Frieda River prospect area, Papua New Guinea: ECONOMIC GEOLOGY, v. 77, p. 592–616.

Whitebread, D.H., and John, D.A., 1992, Geologic map of the Tonopah 1° by 2° quadrangle, central Nevada: U.S. Geological Survey Miscellaneous Field Studies Map MF-1877-A, 1:250,000.

## APPENDIX

### Adularia Sample Descriptions and Locations

Sample locations are shown in Figures 2 and 4.

421-796. Sample from drill hole 421 at a depth of 796 ft; coarse, 1- to 5-mm rhombs along open fracture in Paleozoic rocks; 38° 42.3′ N, 117° 04.7′ W.

D175A. Sample from drill hole D175A at a depth of 1,416 ft; coarse, 0.5- to 1-mm rhombs along fractures in nonwelded, lower part of upper member of tuff of Round Mountain; drill hole is on downthrown side of series of Basin and Range faults that strike northeast across the northwestern edge of the Round Mountain deposit; 38° 42.5′ N, 117° 05.5′ W.

SH. Sample is from outcrop on the now mined away part of Stebbins Hill; sample consists of coarse, 1- to 7-mm rhombs from a late, coxcomb, quartz-adularia vein that cuts the upper, densely welded part of the tuff of Round Mountain; 38° 42.6′ N, 117° 04.6′ W.

SL. Sample is from propylitically altered rock overprinted by potassic alteration in the north wall of the pit at the 5,665-ft level; sample consists of finely intergrown rhombs, ~100 $\mu$m in diameter, and quartz that have replaced groundmass in the lower, nonwelded part of the upper member of the tuff of Round Mountain; 38° 42.2′ N, 117° 04.9′ W.

HGV. Sample is from the wall of the pit at the 6,010-ft level; sample consists of fine, ~0.1- to 0.4-mm, rhombs intergrown with quartz in a vein that contained ~100 oz/t Au; the vein was nearly flat lying and occurred in the transition zone between the lower, nonwelded and upper, densely welded part of the upper member of the tuff of Round Mountain; this area has been removed by mining; 38° 41.9′ N,117° 04.6′ W.

Type II. Sample is from the wall of the pit at the 5,665-ft level; sample consists of coarse, 1- to 3-mm rhombs within (replacing?) pumice fragments of the lower, nonwelded part of the upper member of the tuff of Round Mountain; 38 42.2′ N, 117 04.8′ W.

#3 Stringer. Sample is from an overgrowth vein in the wall of the pit at the 6,080-ft level; sample consists of coarse, 1- to 5-mm grains that nucleated on sanidine phenocrysts in the wall rock, which is the densely welded part of the upper member of the tuff of Round Mountain; 38° 42.3′ N, 117° 05.0′ W.

D8 271. Sample is from drill hole D8 at a depth of 271 ft, which is now in the middle of the pit; sample consists of completely adularized sanidine phenocrysts with inclusions of albite, quartz, smectite, and chlorite(?) from the upper, densely welded part of the upper member of the tuff of Round Mountain; 38° 42.1′ N, 117° 04.7′ W.

H95-51A. Sample is from propylitically altered rock in the north wall of the pit at the 5,835-ft level; sample consists of completely adularized sanidine phenocrysts with inclusions of calcite, albite, quartz, smectite, and chlorite(?) from the upper, densely welded part of the upper member of the tuff of Round Mountain; 38° 42.2′ N, 117° 05.0′ W.